

## RESEARCH ARTICLE

# Minibrain drives the Dacapo-dependent cell cycle exit of neurons in the *Drosophila* brain by promoting *asense* and *prospero* expression

Mirja N. Shaikh, Francisco Gutierrez-Aviño, Jordi Colonques, Julian Ceron\*, Barbara Hämmerle and Francisco J. Tejedor<sup>‡</sup>

## ABSTRACT

A key aim of neurodevelopmental research is to understand how precursor cells decide to stop dividing and commence their terminal differentiation at the correct time and place. Here, we show that *minibrain* (*mnb*), the *Drosophila* ortholog of the Down syndrome candidate gene *DYRK1A*, is transiently expressed in newborn neuronal precursors known as ganglion cells (GCs). *Mnb* promotes the cell cycle exit of GCs through a dual mechanism that regulates the expression of the cyclin-dependent kinase inhibitor Dacapo, the homolog of vertebrate p27<sup>Kip1</sup> (Cdkn1b). *Mnb* upregulates the expression of the proneural transcription factor (TF) *Asense*, which promotes Dacapo expression. *Mnb* also induces the expression of *Prospero*, a homeodomain TF that in turn inhibits the expression of *Deadpan*, a pan-neural TF that represses *dacapo*. In addition to its effects on *Asense* and *Prospero*, *Mnb* also promotes the expression of the neuronal-specific RNA regulator *Elav*, strongly suggesting that *Mnb* facilitates neuronal differentiation. These actions of *Mnb* ensure the precise timing of neuronal birth, coupling the mechanisms that regulate neurogenesis, cell cycle control and terminal differentiation of neurons.

**KEY WORDS:** DYRK1A, Neurogenesis, Neural proliferation, Neural progenitor, Neuronal differentiation, Neuronal precursor

## INTRODUCTION

Cell proliferation, specification and terminal differentiation must be precisely coordinated during brain development in order to ensure the correct balance between the number of cells in different populations and the subsequent formation of functional circuits. When the coordination between these processes is impaired, aberrant tissue development, neuropathologies and tumorigenesis may ensue (Zhu and Skoultschi, 2001; Buttitta and Edgar, 2007; Malumbres and Barbacid, 2009; Hindley and Philpott, 2012).

Given its intermediate complexity and the sophisticated genetic tools available, the larval central nervous system (CNS) of *Drosophila* provides a suitable experimental model in which to study the genetic basis underlying neurodevelopment (Gonzalez, 2007; Sousa-Nunes et al., 2010; Brand and Livesey, 2011; Homem

and Knoblich, 2012). The larval CNS is composed of two brain hemispheres and the ventral ganglia. The primordium of the adult central brain (CB) develops in the medial region of each hemisphere, whereas the adult optic lobes (OLs) develop from the primordia located laterally in the hemispheres (summarized in Fig. S1).

Most OL neurons are generated at the end of larval development from neural progenitors (NPs) called neuroblasts (NBs) that delaminate progressively from two neuroepithelia during the third instar larval period – the OPC (outer proliferation center) and the IPC (inner proliferation center). The OPC is located laterally on the OL surface and it gives rise to the lamina precursor cells (LPCs) and medulla neurons, whereas the IPC, which is located inside the lobe, generates the lobula neurons (Hofbauer and Campos-Ortega, 1990; reviewed by Meinertzhagen and Hanson, 1993; Apitz and Salecker, 2014). The adult CB originates from ~100 NBs located medially in each hemisphere. These NBs are born in the procephalic region during embryogenesis, and, after generating the functional neurons of the larval brain, most of them enter quiescence at the end of embryogenesis. These CB NBs re-enter the cell cycle progressively from the first to third larval instar and they stop proliferating on the first day of pupation (White and Kankel, 1978; Truman and Bate, 1988; Hofbauer and Campos-Ortega, 1990; Ito and Hotta, 1992; Datta, 1995; Ebens et al., 1993).

Based on their cellular and molecular properties, two main types of larval NBs have been described. The ventrally located Type I CB NBs and OPC NBs proliferate like embryonic NBs, although they produce more cells with more restricted fates within each lineage. Thus, they divide asymmetrically several times to generate a new NB and an intermediate progenitor called ganglion mother cell (GMC), which divides terminally to generate two post-mitotic ganglion cells (GCs) that most frequently differentiate into neurons (Ito et al., 1997; Ceron et al., 2001; Colonques et al., 2007). Type II NBs are located in the dorso-posterior medial region and they self-renew by asymmetrical division, budding-off intermediate progenitors that undergo multiple divisions (Bello et al., 2008; Boone and Doe, 2008; Bowman et al., 2008).

Adult mutant *minibrain* (*mnb*) flies have a smaller brain but with no gross alterations in its overall organization (Fischbach and Heisenberg, 1984; Tejedor et al., 1995). This change in size is particularly evident in the ventro-anterior CB and the OL, and is due to neuronal deficits that have been related to altered proliferation in the larval neurogenic centers, particularly in the OPC, suggesting that *Mnb* regulates neural proliferation and neurogenesis during post-embryonic CNS development (Tejedor et al., 1995). Nevertheless, the cellular and molecular mechanisms underlying this phenotype remain mostly unknown.

The *mnb* gene encodes a dual protein kinase that is strongly conserved from insects to humans (reviewed by Galceran et al.,

Instituto de Neurociencias, CSIC and Universidad Miguel Hernandez, Alicante 03550, Spain.

\*Present address: Cancer and Human Molecular Genetics, Bellvitge Biomedical Research Institute – IDIBELL, L'Hospitalet de Llobregat, Barcelona 08908, Spain.

<sup>‡</sup>Author for correspondence (f.tejedor@umh.es)

© F.J.T., 0000-0003-1942-2580

Received 18 December 2015; Accepted 25 July 2016

2003), and it has been implicated in vertebrate neurodevelopment (reviewed by Tejedor and Hämmerle, 2011) and cell cycle regulation (reviewed by Becker, 2012). Interestingly, the truncation of *DYRK1A* in humans causes microcephaly (Møller et al., 2008) and autosomal dominant mental retardation 7 (MRD7; OMIM 614104; van Bon et al., 2011), which is reminiscent of the *mnb* loss-of-function (LoF) phenotype in *Drosophila*. Remarkably, the human *DYRK1A* gene lies in the so-called Down syndrome (DS) critical region on chromosome 21 (Guimerà et al., 1996) and it has been related to several neurodevelopmental pathological aspects of DS (reviewed by Tejedor and Hämmerle, 2011). Thus, the MNB/DYRK1A kinase is currently considered a DS therapeutic target (Becker et al., 2014). Therefore, defining the cellular processes and molecular mechanisms in which MNB/DYRK1A is involved could be crucial for the design of such therapeutic strategies.

There is compelling evidence that Dyrk1A is a crucial regulator of the transition from mitotically active precursors to terminally differentiated neurons in the vertebrate CNS (reviewed by Tejedor and Hämmerle, 2011). In particular, we found that Dyrk1A regulates the cell cycle exit of vertebrate CNS neurons by upregulating the expression of the cyclin-dependent kinase inhibitor (CKI) p27<sup>Kip1</sup> (Cdkn1b) (Hämmerle et al., 2011). Given the strong evolutionary conservation of Mnb/Dyrk1A, we have performed genetic, cellular and molecular analyses in the *Drosophila* larval CNS to unravel the molecular mechanisms underlying this function.

## RESULTS

Given the phenotype of *mnb* mutants, this study focused on the OPC and the ventral-anterior CB.

### Loss of *mnb* function induces overproliferation and cell death

To define the developmental stage at which neuronal deficits are generated in *mnb* mutants, we carried out *in vivo* pulse/chase bromodeoxyuridine (BrdU) labeling experiments (Fig. S2). As a decrease in BrdU<sup>+</sup> cells was only detected when pulses were applied at late larval stages, we concluded that the neuronal deficit of *mnb* flies is mainly generated during late post-embryonic neurogenesis. Indeed, we previously found that changes in the pattern of BrdU labeling were evident in the OL of *mnb* late third-instar larval brains after a 1 h BrdU pulse, although the number of BrdU-labeled cells was often not substantially altered (Tejedor et al., 1995). As we subsequently found the cell cycle of OL NBs to be shorter than 1 h (Ceron et al., 2001), we applied 5–10 min BrdU or 5-ethynyl-2'-deoxyuridine (EdU) pulses *in vitro* to dissected late larval brains. Surprisingly, under these conditions there were more proliferating (BrdU- or EdU-labeled) cells in the larval brain hemispheres of *mnb* mutants than in those of wild-type (*wt*) controls (Fig. 1A–C; Fig. S3), particularly in the OPC and CB. We also observed a similar increase in cells expressing other cell cycle markers such as cyclin E (Fig. 1D,E). Conversely, we found that Mnb overexpression inhibited the proliferation of NBs in the OPC and

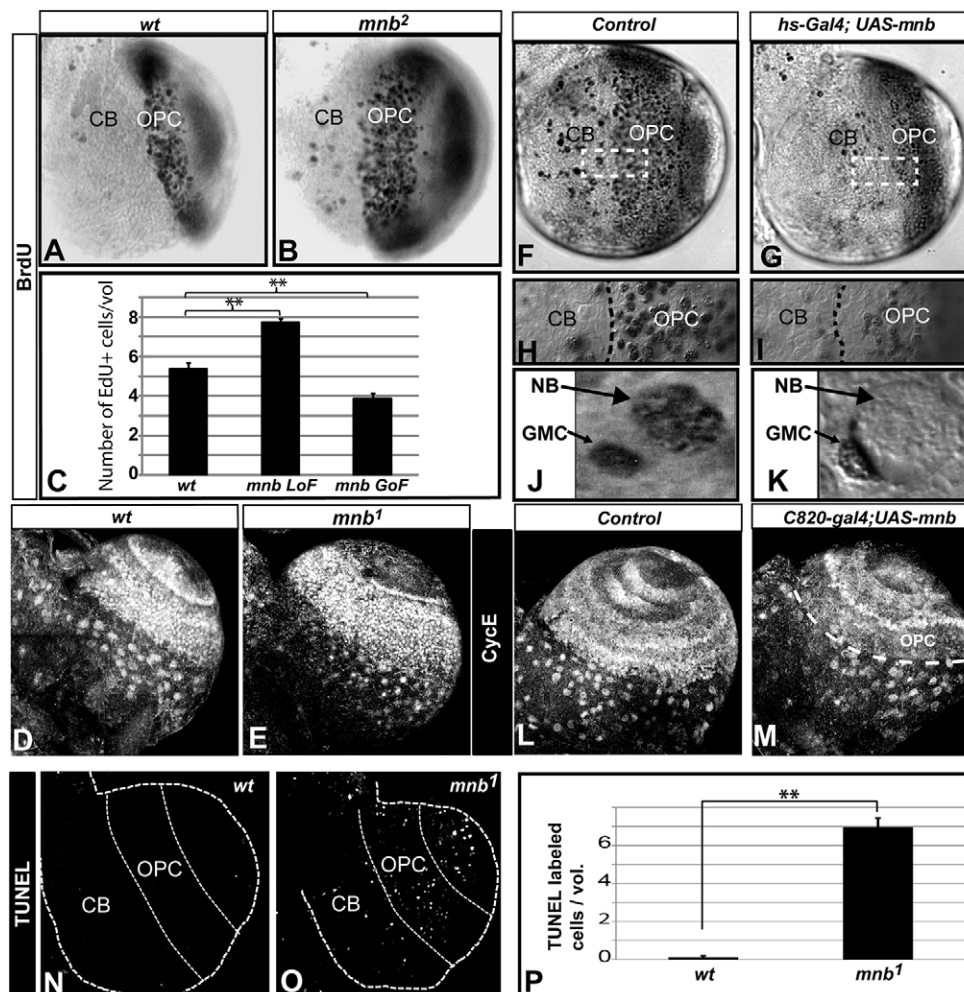


**Fig. 1. Altered proliferation and cell death in the larval brain of *mn<sup>b</sup>* mutants.** (A,B) Immunostaining of brain hemispheres from *wt* and *mn<sup>b2</sup>* late third-instar larvae after a 5 min *in vitro* pulse of BrdU. Note the increased width of the labeled OPC in the mutant compared with the *wt*. (C) Quantification of the density of EdU-labeled cells (cells/10,000  $\mu\text{m}^3$ ) in the OPC of *wt*, *mn<sup>b1</sup>* (LoF) and *mn<sup>b</sup>*<sup>EY14320</sup> (GoF) after a 6 min pulse (four brains; \*\**P*<0.001 by Student's *t*-test). (D,E) More cyclin E-labeled cells are observed in the brain hemisphere of *mn<sup>b1</sup>* compared with the *wt*. (F,G) After an *in vitro* BrdU pulse, the brain hemisphere of a *hs-Gal4;UAS-mnb* larva, which was subjected to a heat shock activation for 10 h, exhibits a strong decrease in BrdU-labeled cells compared with control larvae. (H,I) Higher magnification of the CB/OPC region indicated above. (J,K) High magnifications of representative CB NBs and their daughter GMCs. Note that the *hs-Gal4;UAS-mnb* NB lacks BrdU labeling but GMCs are labeled in both genotypes. (L,M) Fewer cyclin E-labeled cells are observed in the OPC of *c820-Gal4;UAS-mnb* (see driver pattern in Fig. S4) than in the control brain. (N,O) Confocal projections of the brain lobes of *wt* and *mn<sup>b1</sup>* larvae after TUNEL labeling. (P) Density of TUNEL-labeled cells in *wt* and *mn<sup>b1</sup>* larval brain lobes (*n*=5, \*\**P*<0.005 by Mann-Whitney rank sum test). Error bars represent s.d.

CB, reflected by a reduction in the number of BrdU/EdU-labeled cells (Fig. 1C,F–K) and weaker cyclin expression (Fig. 1L,M). These results demonstrate that Mnb negatively regulates neural proliferation during post-embryonic neurogenesis.

The increase in proliferating cells in the late larval brain of *mnb* mutants is intriguing given the neuronal deficits in the adult brain and the decreased BrdU labeling in pulse/chase experiments from late larvae to adults (Fig. S2E,F). This apparent paradox could be explained by a high incidence of apoptotic cell death in the OPC and CB of *mnb* mutants, as determined by terminal deoxynucleotide transferase-mediated dUTP nick-end labeling (TUNEL) analysis (Fig. 1N–P), Acridine Orange staining, electron microscopy (Fig. S5A–D) and activated caspase-3 immunolabeling (not shown).

### ***mnb* is weakly expressed in NBs and transiently upregulated in newborn GCs**

We studied *mnb* expression in the late larval CNS in detail by fluorescence *in situ* hybridization (FISH) and immunohistochemistry (IHC) in combination with markers for NBs/GMCs [Grainyhead (Grh)], mitotic NBs/GMCs [phosphorylated histone-3 (PH3)], newborn GCs [Prospero (Pros); Colonques et al., 2011] and early differentiating GCs/neurons (Elav; Robinow and White, 1991). We found strong *mnb* mRNA expression in scattered OPC and CB cells (Fig. 2A). These cells were located beneath the NB/GMC layers in the OPC and close to CB NBs/GMCs (Grh<sup>+</sup>, PH3<sup>+</sup>) that lacked *mnb* mRNA (Fig. 2C–G), suggesting that *mnb* is mainly expressed by GCs. As the GC markers did not work properly after FISH, this was assessed by IHC with a specific Mnb antiserum that labeled cells throughout the larval CB and OPC (Fig. 2H). This cellular pattern was more extensive than the restricted distribution of *mnb* mRNA-expressing cells, probably reflecting the higher sensitivity of IHC, as the specificity of both patterns was evident by the widespread reduction in *mnb* hypomorph alleles (Fig. 2A,B,H,I). Indeed, consistent with the expression of Mnb in GCs, Mnb immunostaining was detected in the progeny close to each NB, partially overlapping that of Pros and Elav (Fig. 2K). Weak immunolabeling was also observed in NBs (Fig. 2K,L). Hence, *mnb* appears to be weakly expressed in NBs and upregulated in newborn GCs, and the Mnb protein persists as these cells differentiate into neurons and move away from the parental NB (Fig. 2M).

Given this pattern, the cell type on which *mnb* acts to regulate proliferation should be clarified. Interestingly, the excess proliferation in *mnb* mutants was mainly due to an increase in small proliferating (BrdU<sup>+</sup> or EdU<sup>+</sup>) cells located beneath the OPC NBs and near to the CB NBs (Fig. 3B–D), where putative GMCs and GCs lie. This did not appear to be due to supernumerary GMCs because, as in *wt* brains, most frequently, only one midsize Mira<sup>+</sup> cell (GMC) was associated with each CB NB in *mnb* brains (Fig. S5E). Double Mira/EdU labeling revealed three types of EdU-labeled cells in *wt* CB lineages: (1) numerous strong Mira<sup>+</sup> NBs/GMCs (large and medium cells, respectively); (2) pairs of small newborn GCs (weakly expressing Mira) attached to a Mira<sup>+</sup> NB; (3) few Mira<sup>−</sup> cells. Remarkably, there was a much higher proportion of these Mira<sup>−</sup>/EdU<sup>+</sup> cells located near NBs/GMCs in *mnb* mutants, concomitant with a decrease in Mira<sup>+</sup>/EdU<sup>+</sup> NBs/GMCs (Fig. 3E–G). Hence, we concluded that the overproliferation in *mnb* mutants was not due to supernumerary NBs/GMCs but rather to perturbations in the prospective GCs. Indeed, apoptotic (TUNEL<sup>+</sup> and pyknotic) cells were located near Mira<sup>+</sup> CB and OPC NBs/GMCs (Fig. 3H,I; Fig. S5C,D). Together, these results are consistent with the notion that many GCs continue to proliferate

rather than exiting the cell cycle in *mnb* mutants, and that they eventually die by apoptosis.

### **Minibrain regulates the expression of Prospero and its downstream effectors Deadpan and Dacapo**

The data described above strongly suggest that Mnb is required for the cell cycle exit of GCs. Indeed, and as we previously reported for vertebrate Mnb/Dyrk1A (Hämmerle et al., 2011), we found that Mnb regulates the expression of *dacapo* (*dap*; Fig. 4A–C), the *Drosophila* homolog of *p27<sup>Kip1</sup>*. To investigate the molecular mechanisms underlying this regulation, we focused on Pros. This TF is segregated into the GMC during the asymmetric division of embryonic NBs. In GMCs, Pros acts as a key cell fate determinant and it is then immediately downregulated in the newborn GCs (Hirata et al., 1995; Knoblich et al., 1995; Spana and Doe, 1995). By contrast, Pros is expressed weakly (or sub-threshold) in the majority of larval type I NBs and it is robustly upregulated in newborn GCs (Ceron et al., 2001; Colonques et al., 2011), driving their cell cycle exit by promoting *dap* expression (Colonques et al., 2011). We found that Mnb and Pros proteins are co-expressed by GCs although Mnb expression appears to precede that of Pros (Fig. 2L,M). As reported previously, Pros expression precedes that of Elav (Colonques et al., 2011) but it is downregulated earlier than Mnb and Elav as GCs move away from the NB (Fig. 2K,O).

We next investigated whether Mnb regulated *pros* expression. Thus, we found substantially weaker Pros immunolabeling in the OPC and CB of *mnb* LoF mutant brains and, conversely, stronger labeling when Mnb was overexpressed (Fig. 5A–D,G,H; >90% of brains; *n*>50; Fig. S6). This regulation appears to take place at the transcriptional level, as Mnb overexpression increased Pros FISH labeling (Fig. 5E,F; 8/9 brains). Remarkably, the increase in Pros expression in response to *mnb* gain of function (GoF) took place in GCs whereas Pros did not apparently change in NBs, even when Mnb protein accumulated strongly following Gal4 driver induction (Fig. 5I–J’). These results suggest that Mnb promotes *pros* expression in newborn GCs, indicating that Mnb acts upstream of *pros* in driving the cell cycle exit of GCs.

We previously found that the activation of *dap* expression by Pros is mediated through the expression of Deadpan (Dpn; Colonques et al., 2011), an essential pan-neural basic helix-loop-helix (bHLH) TF (Bier et al., 1992) that represses *dap* expression in the larval brain (Wallace et al., 2000). Consistent with Mnb acting upstream of *pros*, *mnb* GoF reduced Dpn immunolabeling (Fig. 6A–B’; 8/11 brains). Remarkably, the overexpression of *mnb* in NBs substantially dampened Dpn expression in the absence of *pros* upregulation (Fig. 6A’–B’), suggesting that Mnb might regulate *dpn* in NBs independently of Pros. Conversely, Dpn expression was enhanced in *mnb* mutants, concomitant with Pros downregulation (Fig. 6C,D; 23/23 brains; quantification in Fig. S7), and small Dpn<sup>+</sup> cells were frequently found beneath the OPC NBs (Fig. 6E,F; 15/23 brains). As these extraneuronal Dpn<sup>+</sup> cells lacked or very weakly expressed Mira (Fig. 6E,F), and no significant increase in Dpn<sup>+</sup> NBs was seen in the CB (Fig. 6G), *dpn* appears to be upregulated in prospective GCs of *mnb* mutants without transforming them into NBs.

### **Mnb promotes the expression of Asense**

The observation that Mnb GoF suppresses NB proliferation (Fig. 1) without inducing Pros expression (Fig. 5I; Fig. 6B’) strongly suggests that Mnb can promote cell cycle exit by an additional mechanism independent of Pros. Thus, we focused our attention on Asense (Ase), a bHLH TF of the *achaete-scute* proneural gene



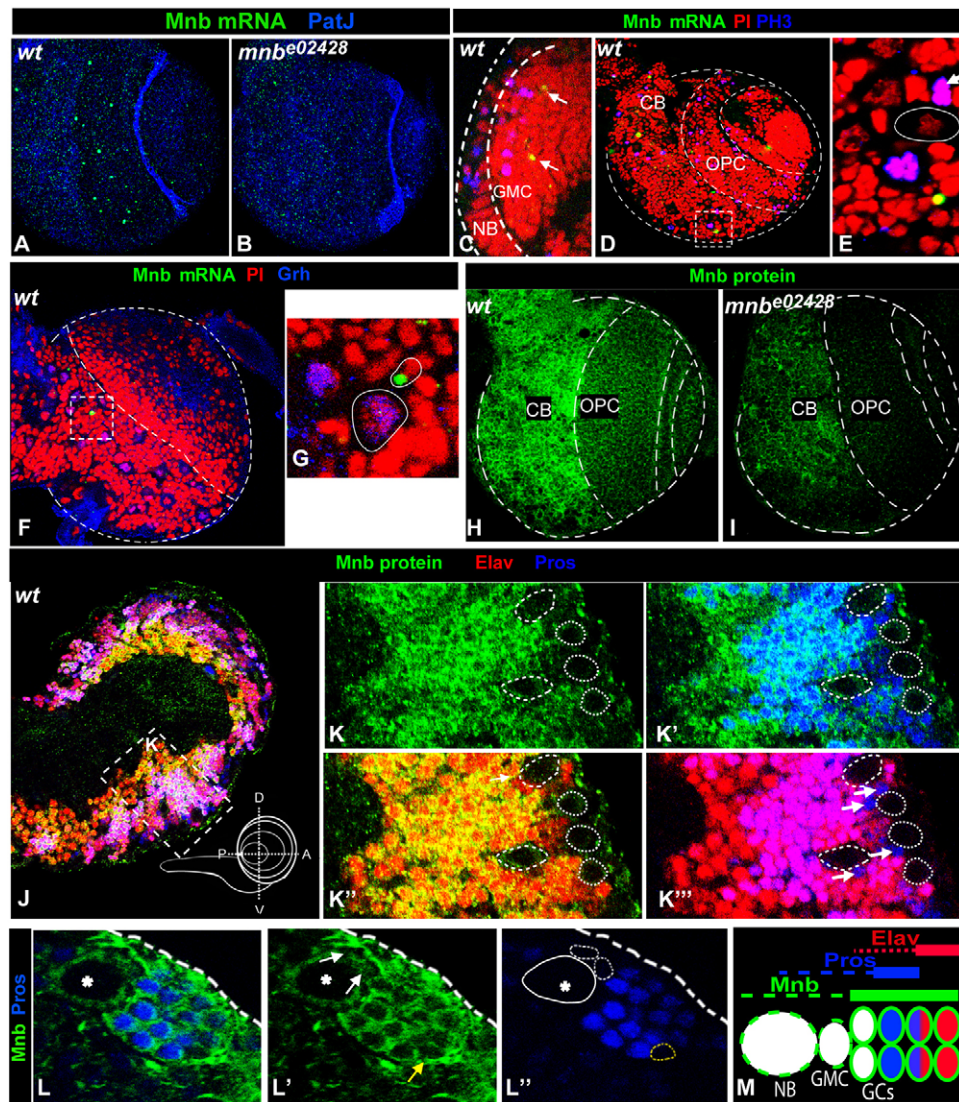


**Fig. 2. Cellular expression of Mnb in the larval brain lobes.** (A–G) Analysis of *mnb* mRNA expression by FISH in the late larval brain. (A,B) Projection of serial confocal images from one brain lobe of a *wt* larva (A) showing numerous scattered Mnb-labeled cells in the OPC and CB, which are substantially fewer in a *mnb<sup>e02428</sup>* larva (B). PatJ labels the OPC NE. (C) Single confocal section at the level of the OPC showing the presence of two cells expressing *mnb* mRNA (arrows) below the layer of the mitotic (PH3<sup>+</sup>) cells: NBs located at the surface and GMCs beneath them. Nuclei are stained with propidium iodide (PI). (D) A single confocal section of a brain lobe showing PH3 and *mnb* mRNA labeling. (E) Higher magnification of the CB cell cluster indicated in D showing a single cell expressing *mnb* mRNA. Note that neither the large mitotic NB (PH3<sup>+</sup>) nor the mitotic GMC (arrow) close to a non-mitotic NB (circle) exhibited *mnb* labeling. (F) A single confocal section of a brain lobe showing *mnb* mRNA, as well as Grh and PI labeling. (G) Higher magnification of the CB cell cluster highlighted in F showing a small cell expressing *mnb* mRNA near a large Grh<sup>+</sup> NB (both circled). (H,I) Confocal image of a *wt* brain lobe (H) showing Mnb immunostaining, which is substantially decreased in a *mnb<sup>e02428</sup>* lobe (I). (J) Lateral confocal image of a brain immunostained for Mnb, Pros and Elav. The scheme indicates its orientation (A, anterior; D, dorsal; P, posterior; V, ventral). (K–K'') Higher magnification of the ventro-anterior region boxed in J. Note that NBs deprived of Elav and Pros express Mnb weakly, whereas Mnb, Pros and Elav are widely co-expressed in the progeny. Nevertheless, GCs located far from the NBs express Mnb and Elav but not Pros, and there are a few Pros<sup>+</sup>/Elav<sup>−</sup> cells (arrows) located near to the NBs. (L–L'') Confocal image of a CB NB (asterisk) and its progeny. Note the absence of Pros in two small cells expressing Mnb (white arrows and dashed circles) near the NB, and in one small cell located far from it (yellow arrow and dashed circle). (M) Schematic summary of the sequential expression of Mnb, Pros and Elav in NB progeny.

complex (Campuzano et al., 1985) that is involved in OL development (Gonzalez et al., 1989). Although Ase is extensively used as a marker of larval NBs, it has intriguingly been reported to promote the expression of *dap* in the larval brain (Wallace et al., 2000). Interestingly, we found that in addition to its expression in NBs (Dpn<sup>+</sup> cells) Ase was also expressed strongly by newborn GCs in the OPC, as identified by their position inside the OL, their lack of Dpn and the co-expression of Pros (Fig. 7A,B). In the CB, Ase is expressed in scattered cell clusters that contain one NB (Dpn<sup>+</sup>, Mira<sup>+</sup>) and two or four small neighboring Dpn<sup>−</sup>/Mira<sup>−</sup> cells

(Fig. 7A,C,D). Accordingly, these small Ase<sup>+</sup> cells appear to be newborn GCs. Nevertheless, and unlike in the OPC, these cells lacked Pros and Elav or expressed them very weakly (Fig. 7C). Notably, these small Ase<sup>+</sup> cells accumulated more Ase than mitotic NBs and GMCs (Fig. 7D,E). Together, these results strongly suggest that *ase* expression is downregulated during NB division, upregulated in newborn GCs and quickly downregulated again.

These results prompted us to assess the possible regulation of *ase* expression by Mnb. Thus, the overexpression of Mnb in NBs (*c831-Gal4* driver, 8/15 brains) and GCs (*pros-Gal4* driver, 7/14 brains;



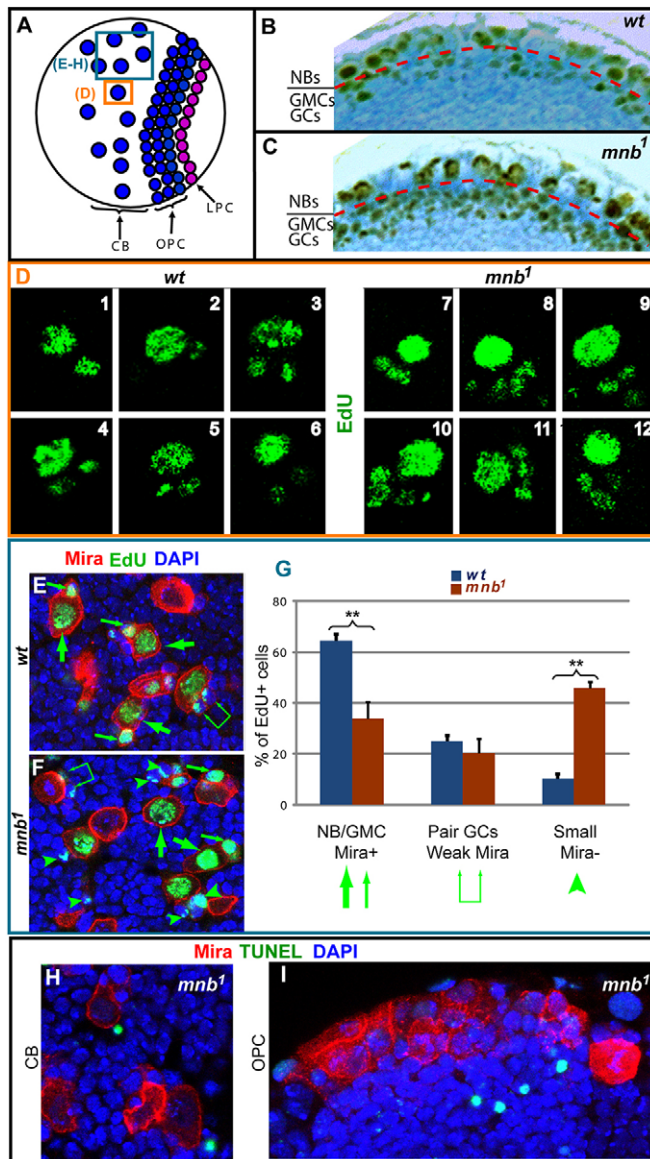


**Fig. 3. Cell phenotype of *mnb* mutants.** (A) Scheme of a brain lobe indicating the regions where the images were taken. (B,C) Partial view of plastic sections at the level of the OPC from immunostained brains of *wt* and *mnb<sup>1</sup>* larvae after a 5 min BrdU pulse. Note the increase in the number of small BrdU-labeled cells located beneath (red line) the superficial NBs in the *mnb* tissue. (D) High magnification views of six representative EdU-labeled CB NB lineages of *wt* and *mnb<sup>1</sup>* larvae after a 6 min EdU pulse. Note the increased number of small labeled cells near a large NB in most *mnb* lineages. (E,F) View of CB lineages of *wt* and *mnb<sup>1</sup>* larvae after a 6 min EdU pulse immunostained for Mira and counterstained with DAPI. Note the increase in small BrdU<sup>+</sup>/Mira<sup>-</sup> cells (arrowheads, putative GCs) in the *mnb* tissue compared with the control. (G) Quantification of three types of labeled cells (symbols used in E are indicated below the graph) in EdU/Mira immunostained *wt* and *mnb<sup>1</sup>* larval brains ( $n=5$ ,  $**P<0.001$  by Student's *t*-test). Error bars represent s.d. (H,I) Representative views of OPC and CB lineages of *mnb<sup>1</sup>* larval brains TUNEL stained, immunostained for Mira and counterstained with DAPI. Note that TUNEL-labeled cells lack Mira.

see driver pattern in Fig. S4C,D) substantially enhanced Ase protein labeling (Fig. 8A–C; quantification in Fig. S8A) without apparently increasing the number of Ase<sup>+</sup> GCs (Fig. 8D,E). Conversely, we found a strong decrease in Ase protein in *mnb* LoF mutants (Fig. S8D–G), both in NBs and newborn GCs (Fig. 8F,G; 9/19

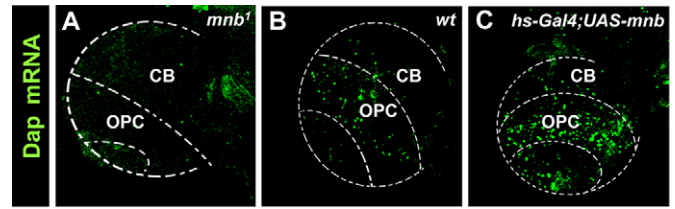


**Fig. 4. Mnb promotes the expression of *dacapo*.** (A–C) Partial confocal projections through the brain lobes of *wt*, *mnb<sup>1</sup>* and *hs-Gal4;UAS-mnb* larvae showing FISH labeling of *dap* mRNA. Note the increase in *dap* labeling in the *hs-Gal4;UAS-mnb* brain lobe and its decrease in the *mnb<sup>1</sup>* lobe compared with the *wt*.

brains). This regulation of Ase expression appeared to occur at the transcriptional level given the enhanced FISH staining in *mnb* GoF mutant brains (Fig. S8B,C; 13/15 brains).

### Mnb promotes *elav* expression in GCs

Because Mnb expression persists in *Elav*<sup>+</sup> GCs that move away from the parental NB after Ase and Pros expression decays (Fig. 2M; Fig. 7F), and *Elav* is a factor required for neuronal differentiation (Robinow et al., 1988; Yao et al., 1993; Lai et al., 2012), we wondered whether Mnb promoted neuronal differentiation of GCs in addition to triggering cell cycle exit. Consistent with this idea, we found weaker *Elav* expression in the GCs of *mnb* LoF mutants (Fig. 8F,G; 14/15 brains; Fig. S9A–D) and after Mnb RNAi (Fig. S9E,F). Conversely, *Elav* expression was enhanced by Mnb overexpression in GCs driven by *elav-Gal4* (data not shown) or *pros-Gal4* (Fig. 8A'–C';  $n=13/15$ ; quantification in Fig. S9G), whereas its overexpression driven by *c831-Gal4* did not induce *Elav* expression in NBs (Fig. S9H,I), even after long-term overexpression that produced prolonged cell cycle arrest (Fig. 8H,I). Accordingly, we concluded that Mnb is necessary and sufficient to promote *Elav* expression in GCs but not in NBs. By contrast, *pros* (Fig. S10; 7/13 brains) or *ase* (Fig. S11; 19/21 brains) GoF did not stimulate or even mildly repress *Elav* expression.

## DISCUSSION

### Minibrain acts upstream of *Asense*, *Prospero*, *Deadpan* and *Dacapo* to regulate the cell cycle exit of *Drosophila* post-embryonic neuronal precursors

The decision of neuronal precursors to exit the cell cycle and commence their terminal differentiation at the right time is a crucial aspect of brain development. CKIs play a central role in the regulation of cell cycle exit during development (Zhu and Skoultschi, 2001; Buttitta and Edgar, 2007). *Drosophila melanogaster* lacks Ink-type CKIs and it has a single Cip/Kip-type CKI, Dap (de Noij et al., 1996; Lane et al., 1996). Hence, like p27<sup>Kip1</sup> in vertebrates (Sherr and Roberts, 1999; Nguyen et al., 2006), Dap plays a central role in controlling the cell cycle exit of CNS neurons. Thus, *dap* LoF mutants are characterized by overproliferation in the larval brain (Wallace et al., 2000), where the expression of *dap* is promoted by Ase and repressed by Dpn. Accordingly, *ase* LoF and *dpn* GoF mutants experience larval brain overproliferation (Wallace et al., 2000). We previously showed that the expression of *dap* in the larval brain is also controlled by Pros and, thus, *dap* is upregulated in newborn GCs in response to the transient expression of Pros, which suppresses *dpn* (Colonques et al., 2011). This is also consistent with the requirement for *pros* to terminate *dpn* expression in embryonic NBs (Vaessin et al., 1991) and to end proliferation of post-embryonic NBs (Maurange et al., 2008).

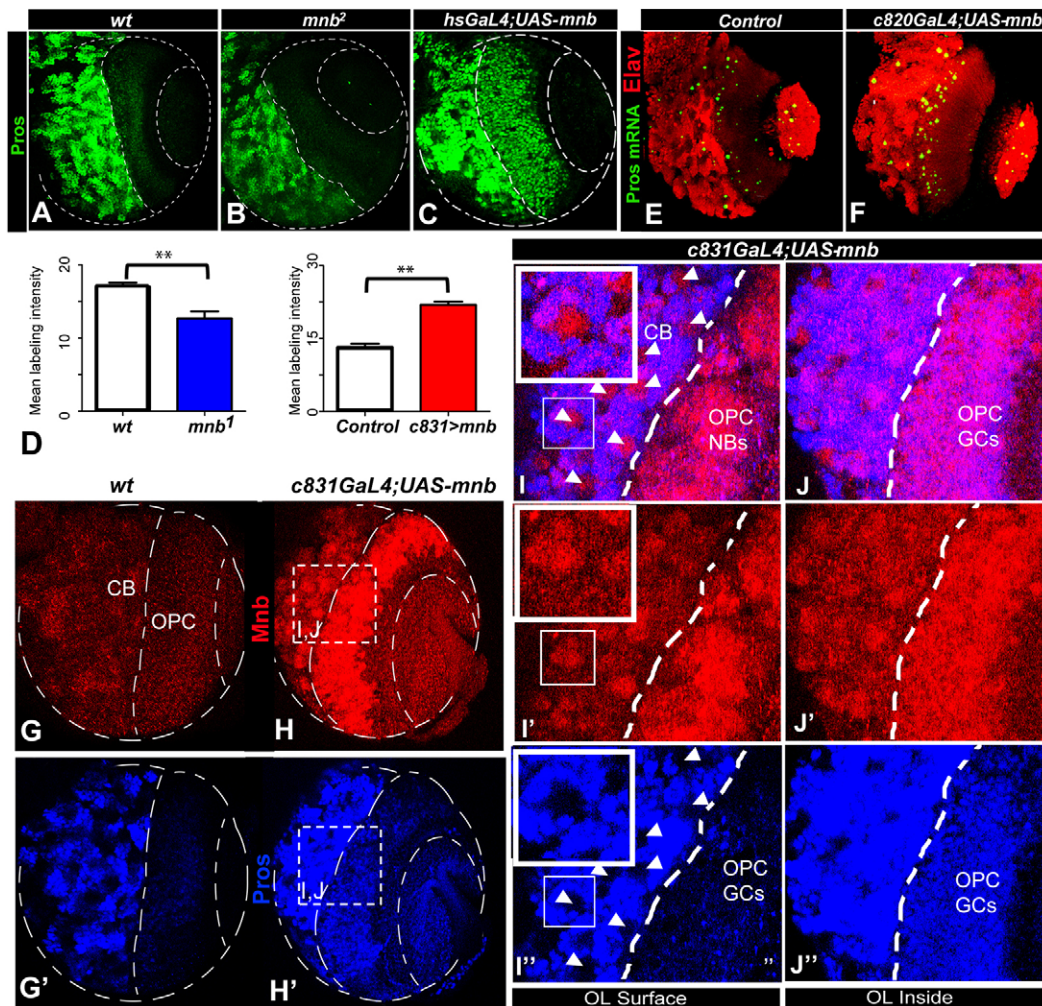


**Fig. 5. Mnb promotes the expression of *prospero* in larval brain GCs.** (A–C) Ventro-anterior confocal projections through the OL of *wt*, *mnb*<sup>2</sup> and *hs-Gal4;UAS-mnb* late third-instar larvae showing Pros protein expression. Note the weaker Pros immunostaining in the *mnb* sample and the increase in *hs-Gal4;UAS-mnb*. (D) Quantification of Pros immunostaining. \*\**P*<0.005 by Student's *t*-test. Error bars represent s.d. (E,F) Confocal projection of *wt* and *c820-Gal4;UAS-mnb* larval brain lobes showing *pros* mRNA and Elav labeling. Note the stronger signal for both *pros* mRNA and Elav in the OPC of the mutant larvae, where *c820-Gal4* drives expression (Fig. S4). (G–J) The overexpression of Mnb in *c831-Gal4;UAS-mnb* brains upregulates Pros in the CB and OPC. Images taken from the surface of the lobe (I–I'), a single NB shown in insets) show that Pros labeling is almost absent from the CB NBs (arrowheads) and OPC NBs that exhibit strong Mnb immunolabeling. By contrast, OPC cell progeny located deeper in the OL (J–J') display strong Pros induction.

We show here that *mnb* inhibits proliferation in the larval brain, where it is expressed weakly in NBs and more strongly in newborn GCs shortly after division of the GMC. Mnb was seen to be necessary and sufficient to promote *pros* expression in GCs, and, consequently, to upregulate *dap* expression. We also found that Mnb promotes *ase* expression in newborn GCs. Thus, Mnb can upregulate *dap* expression through two convergent mechanisms mediated by Ase and Pros (summarized in Fig. 9). Redundant mechanisms regulate cell cycle exit in a number of organisms (reviewed by Buttitta and Edgar, 2007), yet as Ase and Pros are expressed sequentially in GCs, they may also play different roles. Indeed, Ase and Pros appear to regulate antagonistically several gene clusters in gene expression arrays (Southall and Brand, 2009). Thus, we speculate that after the downregulation of *ase* in newborn GCs, Pros helps to maintain *dap* expression, avoiding re-entry of these neuronal precursors into the cell cycle and facilitating their terminal differentiation.

Given the key roles of Dpn in the specification, self-renewal and proliferation of larval NBs (San-Juán and Baonza, 2011; Zhu et al.,

2012), the capacity of Mnb to repress *dpn* expression in NBs independently of *pros* might explain the arrest of proliferation induced by Mnb overexpression in NBs. Hence, Mnb may participate in the control of larval NB proliferation, an issue that merits further study. However, it appears unlikely that Mnb significantly influences NB/GMC specification. Together, our data fit best with the idea that the main actions of Mnb leading to cell cycle exit and terminal differentiation take place in newborn GCs. Accordingly, many of these GCs fail to withdraw correctly from the cell cycle in *mnb* mutants, continuing to proliferate rather than differentiating into neurons, and ultimately dying, possibly explaining the neuronal deficits in the adult *mnb* mutant brain (Fischbach and Heisenberg, 1984; Tejedor et al., 1995).

#### The role of Mnb/Dyrk1A in the cell cycle exit of neurons is evolutionarily conserved

We previously found that Dyrk1A, the mammalian ortholog of *mnb*, is also transiently expressed in newborn neuronal precursors in the embryonic mouse brain (Hämmerle et al., 2008). Furthermore,



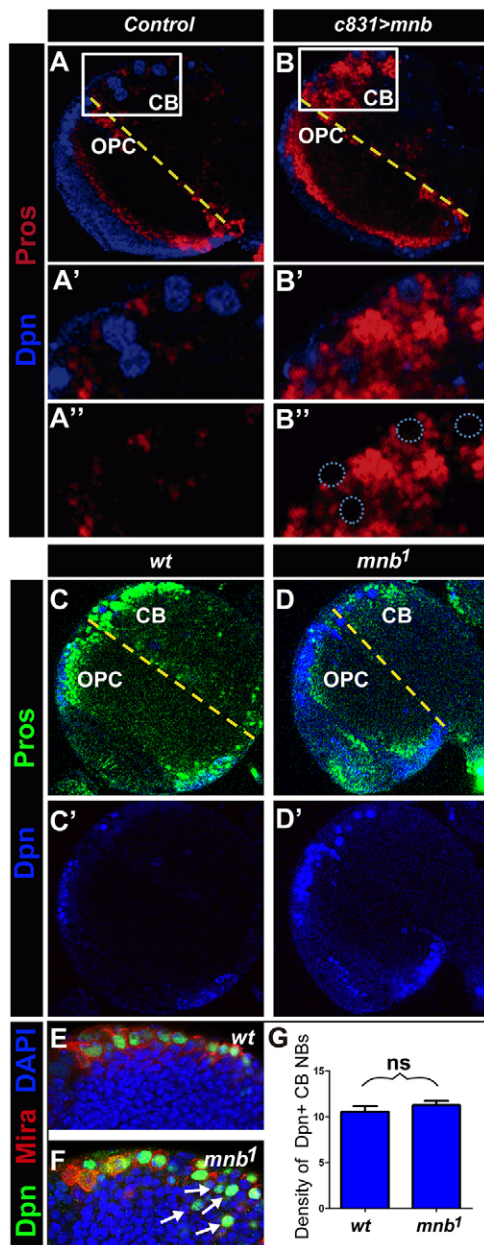


**Fig. 6. Mnb represses the expression of *deadpan*.** (A–D') Single confocal images through one lobe of *wt*, *mnb1*, *UAS-mnb* (Control) and *c831-Gal4; UAS-mnb* late larval brains showing Dpn and Pros protein expression. Note the opposite effects on Dpn and Pros labeling in the GoF versus LoF *mnb* mutant brains. A', A'', B' and B'' show higher magnifications of the boxed areas of the CB shown in A and B. Note the increase in Pros labeling in the GCs surrounding NBs in the *c831>mnb* tissue whereas NBs with no or weak Dpn labeling (dotted circles) also lack Pros labeling. (E,F) Higher magnification of equivalent OPC areas in *wt* and *mnb1* larval brains immunostained for Dpn and Mira, and counterstained with DAPI. Note the stronger Dpn labeling in NBs (Dpn<sup>+</sup>/Mira<sup>+</sup>) at the surface and the presence of small ectopic Dpn<sup>+</sup>/Mira<sup>+</sup> cells (arrows) inside the OPC of *mnb1*. (G) Quantification of the density of Dpn-labeled CB NBs in *wt* and *mnb1* larval brains ( $n=4$ ; ns, not significant;  $P>0.1$  by Student's *t*-test). Error bars represent s.d.

Mnb/Dyrk1A is necessary and sufficient for *p27<sup>Kip1</sup>* expression in the chick and mouse embryo (Hämmerle et al., 2011), strongly suggesting an evolutionarily conserved function in the cell cycle exit of CNS neurons.

Abundant data from diverse experimental systems have implicated Prox1, the vertebrate ortholog of Pros (Oliver et al.,

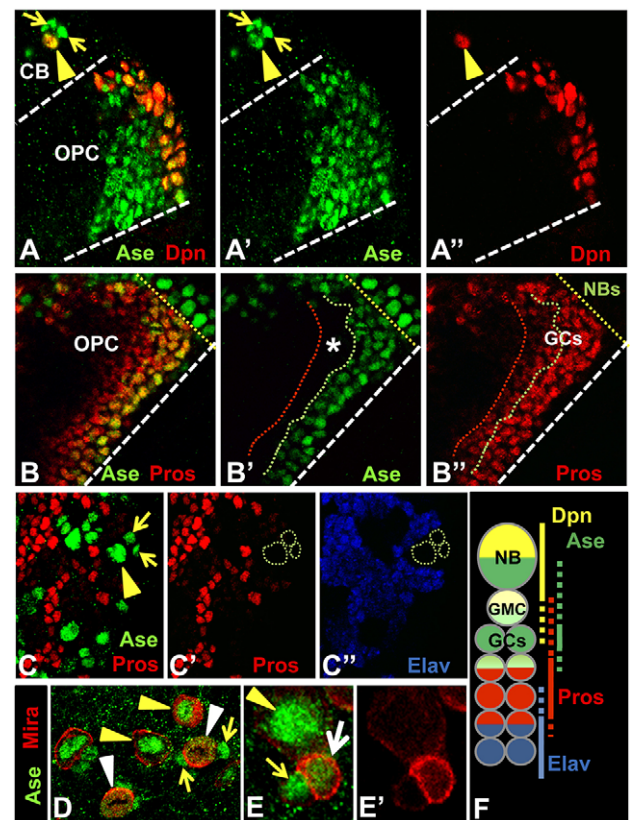


**Fig. 7. Asense is expressed transiently in newborn GCs.** (A–A'') High-magnification view of the OPC in a *wt* larval brain lobe immunolabeled for Ase and Dpn. Ase is expressed by NBs (Dpn<sup>+</sup>) at the surface, as well as by small Dpn<sup>-</sup> cells deep inside the OPC. A nearby CB cluster is also stained for Ase in the NB (Dpn<sup>+</sup>, arrowhead) as are two small adjacent Dpn<sup>-</sup> cells (arrows). (B–B'') Similar view showing NBs (Ase<sup>+</sup>/Pros<sup>-</sup>) at the surface, and co-expression of Pros and Ase in GCs located beneath the NBs. Those GCs located much deeper inside the OPC (between the red and green dotted lines, asterisk) are Ase<sup>-</sup>/Pros<sup>+</sup>. (C–C'') Confocal section of CB lineages showing Ase, Elav and Pros immunolabeling. Note that all small Ase<sup>+</sup> cells (arrows) near NBs (large Ase<sup>+</sup>, arrowhead) are Pros<sup>-</sup>/Elav<sup>-</sup>. (D–E') Confocal section of CB lineages showing Ase and Mira immunolabeling. The Ase signal is weak in mitotic NBs (asymmetric Mira, white arrowheads) compared with interphase NBs (yellow arrowheads, symmetric Mira), and in the small daughter Ase<sup>+</sup> cells (yellow arrows). (E) A recently segregated GMC (Mira<sup>+</sup>, white arrow) with a weaker Ase signal than the parental interphase NB (yellow arrowhead) and a GC (Ase<sup>+</sup>/Mira<sup>-</sup>, yellow arrow). (F) Schematic summary of the sequential expression in a NB lineage.

1993), in cell cycle exit, neuronal differentiation and tumorigenesis (reviewed by Elsir et al., 2012). Remarkably, Prox1 suppresses proliferation by inducing *p27<sup>Kip1</sup>* expression in neuroblastoma cells (Foskolou et al., 2013). Similarly, Dpn is a homolog of the vertebrate Hes TFs that fulfill essential roles in proliferation and specification of neural stem cells (Kageyama et al., 2008). Ascl1 (also known as Mash1), the closest Ase homolog, is a major regulator of vertebrate neurogenesis and, like Ase at the NB to GC transition, *Ascl1* is expressed in an oscillatory manner in the transition from NPs to neuronal precursors (Imayoshi et al., 2013). Also, like Ase, genome-wide characterization of Ascl1 target genes identified both positive and negative regulators of the cell cycle (Castro et al., 2011). Indeed, *Ascl1* LoF in mice is associated with neuronal deficits, whereas its overexpression in NPs induces cell cycle exit and neuronal differentiation (reviewed by Bertrand et al., 2002; Castro and Guillemot, 2011). Remarkably,

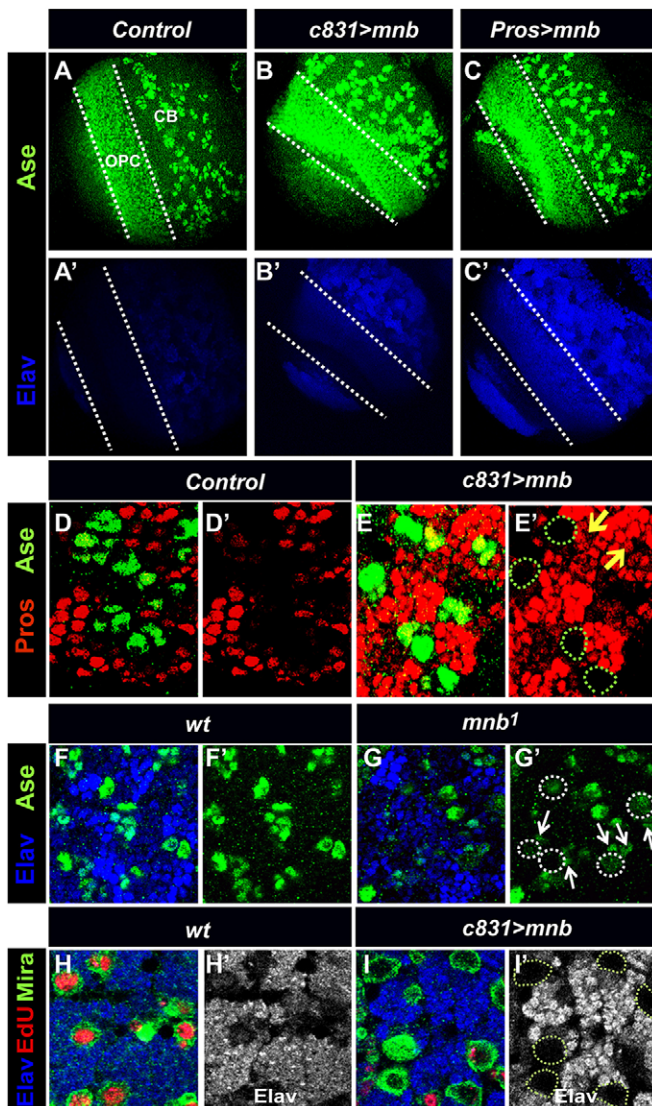


**Fig. 8. Mnb promotes the expression of *asense* and *elav*.** (A–C') Confocal images of brain lobes from *c831-Gal4;UAS-mnb* and *pros-Gal4;UAS-mnb* late larvae showing the increase in Ase and Elav immunolabeling in the OPC and CB relative to the controls. (D–E') High magnification views of equivalent CB areas in control and *c831-Gal4;UAS-mnb* larvae. Note the increase in intensity of Pros labeling and in the number of Pros<sup>+</sup> cells in *c831>mnb*, although most NBs (large Ase<sup>+</sup> cells/dotted green lines) lack Pros. By contrast, stronger Ase labeling can be observed in both NBs and newborn GCs (those near to NBs) but there are very few Pros<sup>+</sup>/Ase<sup>+</sup> cells (arrows). (F–G') Higher magnification of equivalent CB areas from *wt* and *mnb<sup>1</sup>* brains showing the decrease in Elav staining. Ase immunostaining is also much weaker in many NBs (dotted circles) and in most GCs (arrows). (H–I') Equivalent CB areas from *wt* and *c831-Gal4;UAS-mnb* brains immunostained with Mira, EdU and Elav after induction of Mnb for 24 h followed by a 30 min EdU pulse. In the control sample, most NBs (Mira<sup>+</sup>) are EdU<sup>+</sup>/Elav<sup>−</sup>, whereas in the *c831>mnb* lobe most NBs lack EdU as well as Elav (dotted circles).

the expression of *Ascl1* is sufficient to induce neuronal differentiation of uncommitted mammalian cells *in vitro*, preceded by the expression of *p27<sup>Kip1</sup>* (Farah et al., 2000). Moreover, *p27<sup>Kip1</sup>* is required for *Ascl1*-induced neurogenesis in *Xenopus* embryos (Ali et al., 2014). Interestingly, *Ascl1* and *Prox1* expression are regulated at the transition from NP proliferation to terminal differentiation in the rodent forebrain (Torii et al., 1999). Therefore, it will be interesting to determine whether *Ascl1* and

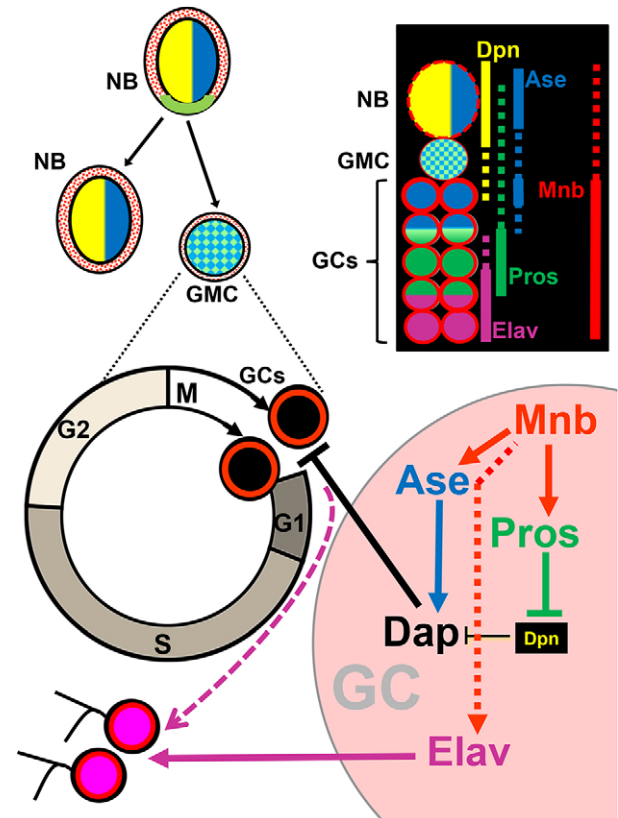


**Fig. 9. Summary of the regulatory mechanisms downstream of Mnb that control cell cycle exit and neuronal differentiation of postembryonic GCs.** The black box scheme summarizes the sequential gene expression involved in GC cell cycle exit and differentiation according to current and previous results (Ceron et al., 2001; Colonques et al., 2011). Our data fit with the following regulatory model. NBs strongly express Ase and Dpn, and they weakly express Mnb and Pros. After GMC division, Mnb expression is upregulated in the newborn GCs, first augmenting the expression of *ase* and immediately afterwards, that of *pros*. Ase then promotes *dap* expression and Pros suppresses the expression of *dpn*, thereby de-repressing Dap expression. These converging actions yield a high level of Dap, which induces cell cycle exit of GCs. Subsequently, Mnb persists in the GCs after *ase* and *pros* are downregulated and promotes Elav expression by an unknown mechanism, thereby stimulating neuronal differentiation.

*Prox1* act downstream of *Dyrk1A* to regulate the cell cycle exit of vertebrate CNS neurons.

In contrast to the anti-proliferative effect of Mnb in the CNS of *Drosophila* described here, Mnb is thought to promote the growth of *Drosophila* imaginal discs by regulating the Salvador-Warts-Hippo pathway (Degoutin et al., 2013). These contrasting data may reflect the different functions of Mnb in neural and non-neural *Drosophila* progenitor cells. Intriguingly, the vertebrate Mnb/*Dyrk1A* orthologs (Yabut et al., 2010; Litovchick et al., 2011; Hämmerle et al., 2011; Soppa et al., 2014) and other DYRKs (reviewed by Becker, 2012) appear to act as cell cycle repressors in both neural and non-neural mammalian cells.

#### A possible role of Mnb in coupling cell cycle exit and neuronal differentiation

Cell cycle exit and terminal cell differentiation must be tightly coupled during normal development in order to avoid premature differentiation of proliferating progenitors, and to ensure that terminally differentiating cells become refractory to proliferative signals. The capacity of Mnb to upregulate *elav* suggests that Mnb



may promote the differentiation of newborn GCs in addition to driving cell cycle exit. Elav is a neuronal-specific RNA-binding protein required for the differentiation and maintenance of neurons in *Drosophila* (Robinow et al., 1988; Yao et al., 1993; Lai et al., 2012) where it regulates alternative splicing (Koushika et al., 1996; Lisbin et al., 2001). Interestingly, Mnb/Dyrk1A has also been implicated in the regulation of splicing (Álvarez et al., 2003; de Graaf et al., 2004; Shi et al., 2008) and, thus, it is tempting to speculate that Mnb can promote neuronal differentiation through mechanisms affecting RNA regulation.

Given that Mnb is expressed in differentiating GCs after *ase* and *pros* are downregulated, and that, unlike Pros or Ase GoF alone, it promotes the expression of Elav, Mnb could regulate Elav expression independently of Pros and Ase. This might also explain why *mnb* mutants exhibit both GC overproliferation and cell death, whereas only overproliferation is evident in *ase* and *pros* mutants (Wallace et al., 2000; Colonques et al., 2011). Nevertheless, we cannot rule out the possibility that Pros and Ase, together or along with additional factors, may act downstream of Mnb to promote Elav expression.

Together, our data suggest a possible role for Mnb in coupling the termination of GC proliferation by regulating *dap* via Ase and Pros, to the beginning of neuronal differentiation through Elav (and possibly other unknown factors). We previously found that Mnb/Dyrk1A is also transiently expressed in vertebrate neuronal precursors (Hämmerle et al., 2002; Hämmerle et al., 2008), where it promotes both cell cycle exit and neuronal differentiation (Hämmerle et al., 2011). Thus, our data suggest an evolutionarily conserved function that couples cell cycle exit to neuronal differentiation during CNS neurogenesis.

### Possible implications for Down syndrome

The presence of the human *mnb* ortholog *DYRK1A* on chromosome 21 (Guimerà et al., 1996), its overexpression in the developing DS brain (Guimera et al., 1999) and its neurodevelopmental functions have implicated this kinase in DS neuropathology (reviewed by Tejedor and Hämmerle, 2011). Among the neurological alterations caused by DS, we must highlight the neuronal deficit in certain brain regions (Becker et al., 1991). As neural proliferation and neurogenesis are altered in the forebrain of fetuses with DS and in embryos of DS mouse models, this deficit most likely originates during early brain development (reviewed by Contestabile et al., 2010). Hence, we hypothesized that the overexpression of *DYRK1A* in fetuses with DS could cause premature cell cycle exit and differentiation, and, consequently, the depletion of NP pools, thereby contributing to the neuronal deficits in DS (Tejedor and Hämmerle, 2011). Remarkably, a specific inhibitor of the Mnb/Dyrk1A kinase rescues the premature neuronal differentiation phenotype displayed by NPs isolated from DS mouse brains (Mazur-Kolecka et al., 2012).

In conjunction, our results support the idea that Mnb acts on multiple factors that link the mechanisms regulating neurogenesis, cell cycle control and terminal differentiation, ensuring the precise generation of neurons. Genetic modifications of *Mnb/Dyrk1A*, such as those that occur in microcephaly and DS, will disrupt this precise coordination, altering neurogenesis during brain development.

## MATERIALS AND METHODS

### *Drosophila* strains

Fly stocks (*Drosophila melanogaster*) were raised at 25°C on standard medium, except for flies carrying the Gal4/UAS transgenes, which were kept at 17°C until the time of induction when the temperature was raised to

29°C. We generated several transgenic *w; P[w<sup>+</sup>UAS-mnb]* lines by inserting the coding regions of the *mnb* C transcript (Tejedor et al., 1995) into the pUAST plasmid (Brand and Perrimon, 1993) following standard procedures for embryo transformation. The *wt* strains used were *Berlin* and *Oregon-R*. The following *mnb* alleles were used: *mnb<sup>1</sup>*, *mnb<sup>2</sup>*, *mnb<sup>3</sup>*, *mnb<sup>ey02428</sup>*, *mnb<sup>ey14320</sup>* and *UAS-mnb RNAi* (see details in Table S1). Other mutant stocks were: *pros-Gal4.C20*, *UAS-pros* (F. Matsuzaki, Center for Developmental Biology, Kobe, Japan); *Elav-Gal4*, *UASmCD8::GFP*, *hs-Gal4/TM3* (Bloomington Stock Center); *c820-Gal4*, *c831-Gal4* (Manseau et al., 1997); *UAS-ase* (Y. N. Yan, Howard Hughes Medical Institute, San Francisco, USA).

### Gain of function of *minibrain*

The overexpression of Mnb was carried out by crossing *UAS-mnb* flies with several Gal4 drivers. These flies were grown at 16–18°C from embryo until mid-late third instar larvae. Tests were carried out to assess leaky activation of the driver. Only drivers that remain silent during the low temperature period were used. Then, the temperature was shifted to 29°C for 8–12 h for the activation of Gal4. In the case of crosses with the *hs-Gal4* driver, this last step was preceded by a heat shock by immersing the larvae tubes in a water bath at 37°C for 20 min.

### Generation of RNAi clones

*hsp70-Flp; Actin5C <yellow, [stop]> Gal4, UAS-GFP* (for control clones) or *hsp70-Flp; Actin5C <yellow, [stop]> Gal4, UAS-GFP / UAS-mnb RNAi* (stock P{KK102642} from the Vienna *Drosophila* RNAi Center) were grown at 17°C until 24 h before pupae formation. Then, a heat shock of 20 min at 37°C was applied and incubation continued at 29°C until wandering larva stage. Brains were dissected and IHC performed as previously described (Colonques et al., 2007; Colonques et al., 2011).

### BrdU and EdU labeling

For *in vivo* pulse/chase BrdU labeling, larvae were fed for 2.5 h with BrdU (pulse) at the desired developmental time and then allowed to develop until (chase) white pupae or 1 day after adult eclosion. *In vitro* BrdU labeling of dissected larval brains was essentially performed as described previously (Tejedor et al., 1995; Ceron et al., 2001) but with BrdU pulses of 5–10 min. For cellular analysis, BrdU-labeled larval brains were embedded in plastic and processed, as described elsewhere (Rogerio et al., 1997). *In vitro* EdU labeling was also carried out by giving pulses of 6–30 min to dissected larval brains followed by IHC analysis. See supplementary Materials and Methods for detailed descriptions.

### Production and purification of Mnb antiserum

We raised an antiserum (MNB-NTH) against the N-terminal region of all Mnb protein isoforms following a procedure similar to that described elsewhere (Tejedor et al., 1995). Its specificity was validated by IHC of *mnb* mutants (Fig. 2H,I). See supplementary Materials and Methods for details.

### Immunohistochemistry

Immunohistochemical analysis of late larval brains was performed as described previously (Ceron et al., 2001; Colonques et al., 2007, 2011). See supplementary Materials and Methods for details of antibodies and quantitative image analysis.

### Fluorescence *in situ* hybridization (FISH)

Digoxigenin (DIG) DNA-labeled probes were synthesized by PCR. For *mnb*, we used either a 237 bp fragment that corresponds to positions 1617–1853 or a 321 bp fragment corresponding to positions 1000–1320 of the *mnb* cDNA sequence (GenBank BT015255). FISH of *Dap* was performed as described elsewhere (Colonques et al., 2011). A DIG-RNA probe for Ase was prepared from a cDNA obtained by subcloning a 0.9 kb cDNA fragment of clone RE15472 (nucleotides 1541–2446) inserted in the pFLC1 vector. Antisense and sense probes were synthesized with T3 and T7 RNA polymerases, respectively. All hybridized probes were detected with a horseradish peroxidase-coupled anti-DIG antibody (Roche), and visualized by tyramide signal amplification (TSA) with Cy2 or Cy3 (Perkin Elmer).

## Analysis of cell death

For TUNEL analysis, larval brains were dissected in cold PBS and immediately fixed with 4% paraformaldehyde/1% Triton X-100 in PBS for 1 h at room temperature. The tissue was then washed sequentially with 0.3% Triton X-100/0.02% Na<sub>2</sub>S<sub>2</sub>O<sub>8</sub> in PBS 3×10 min, once quickly in PBS, then in citrate buffer (pH 6)/0.1% Triton X-100 for 1 min at 65°C and finally with PBS again. The nick-end labeling reaction was performed as recommended by the supplier (Roche). Cell death was also monitored by Acridine Orange staining, electron microscopy and by activated caspase 3 IHC. See supplementary Materials and Methods for details.

## Statistics

Experiments were repeated at least three times. Sample size ( $n$ =number of brains) was adjusted according to the penetrance and variability of phenotype. A minimum of six brains was used in each experiment. Only damaged or disoriented samples were excluded from the analysis.

For statistics, mean and standard deviation (s.d.) values were calculated by standard methods and the statistical significance of differences was determined using the Student's  $t$ -test, one-way ANOVA or the Mann–Whitney Rank Sum test, depending on the experimental characteristics.

## Acknowledgements

We are grateful to J.J. Cabanes and D. Tornero for assistance in generating the transgenic flies, to M.J. Chulia and E. Llorens for expert technical assistance, and to the other lab members for interesting discussions. We are indebted to A. Baonza, H. Bellen, S. Campuzano, C. Doe, C. Gonzalez, I.K. Hariharan, Y.-N. Jan, A. Jarman, F. Matsuzaki, H. Reichert, H. Richardson, S. Selleck, J. Skeath, T. Uemura, H. Vaessin, the VDRC, the Bloomington Stock Center, and the Developmental Studies Hybridoma Bank for providing us with flies, antisera and other molecular tools.

## Competing interests

The authors declare no competing or financial interests.

## Author contributions

M.N.S., F.G.-A., J. Ceron, J. Colonques and B.H. performed experiments and analyzed the data. F.J.T. developed the concepts, performed experiments, analyzed the data and wrote the manuscript.

## Funding

This work was supported by grants from the Dirección General de Investigación Científica y Técnica [BFU2009-08831, BFU2012-38892 to F.J.T.]; the Generalitat Valenciana [ACOMP/2012/047 to F.J.T.]; and the Fundación Inocente Inocente [050666100002 to F.J.T.]. J. Ceron and J. Colonques were recipients of PhD fellowships from the Ministerio de Educación y Ciencia. M.N.S. was recipient of a Santiago Grisolia Fellowship from the Generalitat Valenciana.

## Supplementary information

Supplementary information available online at <http://dev.biologists.org/lookup/doi/10.1242/dev.134338.supplemental>

## References

- Ali, F. R., Cheng, K., Kirwan, P., Metcalfe, S., Livesey, F. J., Barker, R. A. and Philpott, A. (2014). The phosphorylation status of Ascl1 is a key determinant of neuronal differentiation and maturation in vivo and in vitro. *Development* **141**, 2216–2224.
- Álvarez, M., Estivill, X. and de la Luna, S. (2003). DYRK1A accumulates in splicing speckles through a novel targeting signal and induces speckle disassembly. *J. Cell Sci.* **116**, 3099–3107.
- Apitz, H. and Salecker, I. (2014). A challenge of numbers and diversity: neurogenesis in the *Drosophila* optic lobe. *J. Neurogenet.* **28**, 233–249.
- Becker, W. (2012). Emerging role of DYRK family protein kinases as regulators of protein stability in cell cycle control. *Cell Cycle* **11**, 3389–3394.
- Becker, L., Mito, T., Takashima, S. and Onodera, K. (1991). Growth and development of the brain in Down Syndrome. *Prog. Clin. Biol. Res.* **373**, 133–152.
- Becker, W., Soppa, U. and Tejedor, F. J. (2014). DYRK1A: a potential drug target for multiple Down syndrome neuropathologies. *CNS Neurol. Disord. Drug Targets* **13**, 26–33.
- Bello, B. C., Izergina, N., Caussinus, E. and Reichert, H. (2008). Amplification of neural stem cell proliferation by intermediate progenitor cells in *Drosophila* brain development. *Neural Dev.* **3**, 5.
- Bertrand, N., Castro, D. S. and Guillemot, F. (2002). Proneural genes and the specification of neural cell types. *Nat. Rev. Neurosci.* **3**, 517–530.
- Bier, E., Vaessin, H., Younger-Shepherd, S., Jan, L. Y. and Jan, Y. N. (1992). deadpan, an essential pan-neural gene in *Drosophila*, encodes a helix-loop-helix protein similar to the hairy gene product. *Genes Dev.* **6**, 2137–2151.
- Boone, J. Q. and Doe, C. Q. (2008). Identification of *Drosophila* type II neuroblast lineages containing transit amplifying ganglion mother cells. *Dev. Neurobiol.* **68**, 1185–1195.
- Bowman, S. K., Rolland, V., Betschinger, J., Kinsey, K. A., Emery, G. and Knoblich, J. A. (2008). The tumor suppressors Brat and Numb regulate transit-amplifying neuroblast lineages in *Drosophila*. *Dev. Cell* **14**, 535–546.
- Brand, A. H. and Livesey, F. J. (2011). Neural stem cell biology in vertebrates and invertebrates: more alike than different? *Neuron* **70**, 719–729.
- Brand, A. H. and Perrimon, N. (1993). Targeted gene expression as a means of altering cell fates and generating dominant phenotypes. *Development* **118**, 401–415.
- Buttitta, L. A. and Edgar, B. A. (2007). Mechanisms controlling cell cycle exit upon terminal differentiation. *Curr. Opin. Cell Biol.* **19**, 697–704.
- Campuzano, S., Carramolino, L., Cabrera, C. V., Ruiz-Gómez, M., Villares, R., Boronat, A. and Modolell, J. (1985). Molecular genetics of the achaete-scute gene complex of *D. melanogaster*. *Cell* **40**, 327–338.
- Castro, D. S. and Guillemot, F. (2011). Old and new functions of proneural factors revealed by the genome-wide characterization of their transcriptional targets. *Cell Cycle* **10**, 4026–4031.
- Castro, D. S., Martynoga, B., Parras, C., Ramesh, V., Pacary, E., Johnston, C., Drechsel, D., Lebel-Potter, M., Garcia, L. G., Hunt, C. et al. (2011). A novel function of the proneural factor Ascl1 in progenitor proliferation identified by genome-wide characterization of its targets. *Genes Dev.* **25**, 930–945.
- Ceron, J., González, C. and Tejedor, F. J. (2001). Patterns of cell division and expression of asymmetric cell fate determinants in postembryonic neuroblast lineages of *Drosophila*. *Dev. Biol.* **230**, 125–138.
- Colonques, J., Ceron, J. and Tejedor, F. J. (2007). Segregation of postembryonic neuronal and glial lineages inferred from a mosaic analysis of the *Drosophila* larval brain. *Mech. Dev.* **124**, 327–340.
- Colonques, J., Ceron, J., Reichert, H. and Tejedor, F. J. (2011). A transient expression of Prospero promotes cell cycle exit of *Drosophila* postembryonic neurons through the regulation of Dacapo. *PLoS ONE* **6**, e19342.
- Contestabile, A., Benfenati, F. and Gasparini, L. (2010). Communication breaks-Down: from neurodevelopment defects to cognitive disabilities in Down syndrome. *Prog. Neurobiol.* **91**, 1–22.
- Datta, S. (1995). Control of proliferation activation in quiescent neuroblasts of the *Drosophila* central nervous system. *Development* **121**, 1173–1182.
- Degoutin, J. L., Milton, C. C., Yu, E., Tipping, M., Bosveld, F., Yang, L., Bellaiche, Y., Veraksa, A. and Harvey, K. F. (2013). Riquiqui and minibrain are regulators of the hippo pathway downstream of Dachsous. *Nat. Cell Biol.* **15**, 1176–1185.
- de Graaf, K., Hekerman, P., Spelten, O., Herrmann, A., Packman, L. C., Büssow, K., Müller-Newen, G. and Becker, W. (2004). Characterization of cyclin L2, a novel cyclin with an arginine/serine-rich domain: phosphorylation by DYRK1A and colocalization with splicing factors. *J. Biol. Chem.* **279**, 4612–4624.
- de Nooij, J. C., Letendre, M. A. and Hariharan, I. K. (1996). A cyclin-dependent kinase inhibitor, Dacapo, is necessary for timely exit from the cell cycle during *Drosophila* embryogenesis. *Cell* **87**, 1237–1247.
- Ebens, A. J., Garren, H., Cheyette, B. N. R. and Zipursky, S. L. (1993). The *Drosophila* anachronism locus: a glycoprotein secreted by glia inhibits neuroblast proliferation. *Cell* **74**, 15–27.
- Elsir, T., Smits, A., Lindström, M. S. and Nistér, M. (2012). Transcription factor PROX1: its role in development and cancer. *Cancer Metastasis Rev.* **31**, 793–805.
- Farah, M. H., Olson, J. M., Sucic, H. B., Hume, R. I., Tapscott, S. J. and Turner, D. L. (2000). Generation of neurons by transient expression of neural bHLH proteins in mammalian cells. *Development* **127**, 693–702.
- Fischbach, K.-F. and Heisenberg, M. (1984). Neurogenetics and behaviour in insects. *J. Exp. Biol.* **112**, 65–93.
- Foskolou, I. P., Stellas, D., Rozani, I., Lavigne, M. D. and Politis, P. K. (2013). Prox1 suppresses the proliferation of neuroblastoma cells via a dual action in p27-Kip1 and Cdc25A. *Oncogene* **32**, 947–960.
- Galceran, J., De Graaf, K., Tejedor, F. J. and Becker, W. (2003). The MNB/DYRK1A protein kinase: genetic and biochemical properties. In *Advances in Down Syndrome Research* (ed. G. Lubec). J. Neural Trans. Suppl. **67**, pp. 139–148. Wien, New York: Springer publishers.
- Gonzalez, C. (2007). Spindle orientation, asymmetric division and tumour suppression in *Drosophila* stem cells. *Nat. Rev. Genet.* **8**, 462–472.
- Gonzalez, F., Romani, S., Cubas, P., Modolell, J. and Campuzano, S. (1989). Molecular analysis of the asense gene, a member of the achaete-scute complex of *Drosophila melanogaster*, and its novel role in optic lobe development. *EMBO J.* **8**, 3553–3562.
- Guimérà, J., Casas, C., Pucharcós, C., Solans, A., Domènech, A., Planas, A. M., Ashley, J., Lovett, M., Estivill, X. and Pritchard, M. A. (1996). A human homologue of *Drosophila* minibrain (MNB) is expressed in the neuronal regions affected in Down syndrome and maps to the critical region. *Hum. Mol. Genet.* **5**, 1305–1310.



- Guimera, J., Casas, C., Estivill, X. and Pritchard, M. (1999). Human minibrain homologue (MNB/DYRK1): characterization, alternative splicing, differential tissue expression, and overexpression in Down syndrome. *Genomics* **57**, 407-418.
- Hämmerle, B., Vera-Samper, E., Spreicher, S., Arencibia, R., Martínez, S. and Tejedor, F. J. (2002). Mnb/Dyrk1A is transiently expressed and asymmetrically segregated in neural progenitor cells at the transition to neurogenic divisions. *Dev. Biol.* **246**, 259-273.
- Hämmerle, B., Elizalde, C. and Tejedor, F. J. (2008). The spatio-temporal and subcellular expression of the candidate Down syndrome gene Mnb/Dyrk1A in the developing mouse brain suggests distinct sequential roles in neuronal development. *Eur. J. Neurosci.* **27**, 1061-1074.
- Hämmerle, B., Ulin, E., Guimera, J., Becker, W., Guillemot, F. and Tejedor, F. J. (2011). Transient expression of Mnb/Dyrk1a couples cell cycle exit and differentiation of neuronal precursors by inducing p27KIP1 expression and suppressing NOTCH signaling. *Development* **138**, 2543-2554.
- Hindley, C. and Philpott, A. (2012). Co-ordination of cell cycle and differentiation in the developing nervous system. *Biochem. J.* **444**, 375-382.
- Hirata, J., Nakagoshi, H., Nabeshima, Y.-i. and Matsuzaki, F. (1995). Asymmetric segregation of the homeodomain protein Prospero during *Drosophila* development. *Nature* **377**, 627-630.
- Hofbauer, A. and Campos-Ortega, J. A. (1990). Proliferation pattern and early differentiation of the optic lobes in *Drosophila melanogaster*. *Roux's Arch. Dev. Biol.* **198**, 264-274.
- Homem, C. C. and Knoblich, J. A. (2012). *Drosophila* neuroblasts: a model for stem cell biology. *Development* **139**, 4297-4310.
- Imayoshi, I., Isomura, A., Harima, Y., Kawaguchi, K., Kori, H., Miyachi, H., Fujiwara, T., Ishidate, F. and Kageyama, R. (2013). Oscillatory control of factors determining multipotency and fate in mouse neural progenitors. *Science* **342**, 1203-1208.
- Ito, K. and Hotta, Y. (1992). Proliferation pattern of postembryonic neuroblasts in the brain of *Drosophila melanogaster*. *Dev. Biol.* **149**, 134-148.
- Ito, K., Awano, W., Suzuki, K., Hiromi, Y. and Yamamoto, D. (1997). The *Drosophila* mushroom body is a quadruple structure of clonal units each of which contains a virtually identical set of neurons and glial cells. *Development* **124**, 761-771.
- Kageyama, R., Ohtsuka, T. and Kobayashi, T. (2008). Roles of Hes genes in neural development. *Dev. Growth Differ.* **50** Suppl. 1, S97-S103.
- Knoblich, J. A., Jan, L. Y. and Jan, Y. N. (1995). Asymmetric segregation of Numb and Prospero during cell division. *Nature* **377**, 624-627.
- Koushika, S. P., Lisbin, M. J. and White, K. (1996). ELAV, a *Drosophila* neuron-specific protein, mediates the generation of an alternatively spliced neural protein isoform. *Curr. Biol.* **6**, 1634-1641.
- Lai, S.-L., Miller, M. R., Robinson, K. J. and Doe, C. Q. (2012). The Snail family member *Wormiu* is continuously required in neuroblasts to prevent Elav-induced premature differentiation. *Dev. Cell* **23**, 849-857.
- Lane, M. E., Sauer, K., Wallace, K., Jan, Y. N., Lehner, C. F. and Vaessin, H. (1996). Dacapo, a cyclin-dependent kinase inhibitor, stops cell proliferation during *Drosophila* development. *Cell* **87**, 1225-1235.
- Lisbin, M. J., Qiu, J. and White, K. (2001). The neuron-specific RNA-binding protein ELAV regulates neuroglial alternative splicing in neurons and binds directly to its pre-mRNA. *Genes Dev.* **15**, 2546-2561.
- Litovchick, L., Florens, L. A., Swanson, S. K., Washburn, M. P. and DeCaprio, J. A. (2011). DYRK1A protein kinase promotes quiescence and senescence through DREAM complex assembly. *Genes Dev.* **25**, 801-813.
- Malumbres, M. and Barbacid, M. (2009). Cell cycle, CDKs and cancer: a changing paradigm. *Nat. Rev. Cancer* **9**, 153-166.
- Manseau, L., Baradaran, A., Brower, D., Budhu, A., Elefant, F., Phan, H., Philp, A. V., Yang, M., Glover, D., Kaiser, K. et al. (1997). GAL4 enhancer traps expressed in the embryo, larval brain, imaginal discs, and ovary of *Drosophila*. *Dev. Dyn.* **209**, 310-322.
- Maurange, C., Cheng, L. and Gould, A. P. (2008). Temporal transcription factors and their targets schedule the end of neural proliferation in *Drosophila*. *Cell* **133**, 891-902.
- Mazur-Kolecka, B., Golabek, A., Kida, E., Rabe, A., Hwang, Y.-W., Adayev, T., Wegiel, J., Flory, M., Kaczmarek, W., Marchi, E. et al. (2012). Effect of DYRK1A activity inhibition on development of neuronal progenitors isolated from Ts65Dn mice. *J. Neurosci. Res.* **90**, 999-1010.
- Meinertzhagen, I. A. and Hanson, T. E. (1993). The development of the optic lobe. In *The Development of Drosophila melanogaster* (ed. M. Bate and A. Martinez-Arias), pp. 1363-1392. New York: Cold Spring Harbor Laboratory Press.
- Møller, R. S., Kübart, S., Hoeltzenbein, M., Heye, B., Vogel, I., Hansen, C. P., Menzel, C., Ullmann, R., Tommerup, N., Ropers, H.-H. et al. (2008). Truncation of the Down syndrome candidate gene DYRK1A in two unrelated patients with microcephaly. *Am. J. Hum. Genet.* **82**, 1165-1170.
- Nguyen, L., Besson, A., Roberts, J. M. and Guillemot, F. (2006). Coupling cell cycle exit, neuronal differentiation and migration in cortical neurogenesis. *Cell Cycle* **5**, 2314-2318.
- Oliver, G., Sosa-Pineda, B., Geisendorff, S., Spana, E. P., Doe, C. Q. and Gruss, P. (1993). Prox 1, a prospero-related homeobox gene expressed during mouse development. *Mech. Dev.* **44**, 3-16.
- Robinow, S. and White, K. (1991). Characterization and spatial distribution of the ELAV protein during *Drosophila melanogaster* development. *J. Neurobiol.* **22**, 443-461.
- Robinow, S., Campos, A. R., Yao, K. M. and White, K. (1988). The elav gene product of *Drosophila*, required in neurons, has three RNP consensus motifs. *Science* **242**, 1570-1572.
- Rogero, O., Hämmerle, B. and Tejedor, F. J. (1997). Diverse expression and distribution of Shaker potassium channels during the development of the *Drosophila* nervous system. *J. Neurosci.* **17**, 5108-5118.
- San-Juán, B. P. and Baonza, A. (2011). The bHLH factor *deadpan* is a direct target of Notch signaling and regulates neuroblast self-renewal in *Drosophila*. *Dev. Biol.* **352**, 70-82.
- Sherr, C. J. and Roberts, J. M. (1999). CDK inhibitors: positive and negative regulators of G1-phase progression. *Genes Dev.* **13**, 1501-1512.
- Shi, J., Zhang, T., Zhou, C., Chohan, M. O., Gu, X., Wegiel, J., Zhou, J., Hwang, Y.-W., Iqbal, K., Grundke-Iqbal, I. et al. (2008). Increased dosage of Dyrk1A alters alternative splicing factor (ASF)-regulated alternative splicing of tau in Down syndrome. *J. Biol. Chem.* **283**, 28660-28669.
- Soppa, U., Schumacher, J., Florencio Ortiz, V., Pasqualon, T., Tejedor, F. J. and Becker, W. (2014). The Down syndrome-related protein kinase DYRK1A phosphorylates p27(Kip1) and Cyclin D1 and induces cell cycle exit and neuronal differentiation. *Cell Cycle* **13**, 2084-2100.
- Sousa-Nunes, R., Cheng, L. Y. and Gould, A. P. (2010). Regulating neural proliferation in the *Drosophila* CNS. *Curr. Opin. Neurobiol.* **20**, 50-57.
- Southall, T. D. and Brand, A. H. (2009). Neural stem cell transcriptional networks highlight genes essential for nervous system development. *EMBO J.* **28**, 3799-3807.
- Spana, E. and Doe, C. Q. (1995). The prospero transcription factor is asymmetrically localized to the cortex during neuroblast mitosis in *Drosophila*. *Development* **121**, 3187-3195.
- Tejedor, F. J. and Hämmerle, B. (2011). MNB/DYRK1A as a multiple regulator of neuronal development. *FEBS J.* **278**, 223-235.
- Tejedor, F., Zhu, X. R., Kaltenbach, E., Ackermann, A., Baumann, A., Canal, I., Heisenberg, M., Fischbach, K. F. and Pongs, O. (1995). minibrain: a new protein kinase family involved in postembryonic neurogenesis in *Drosophila*. *Neuron* **14**, 287-301.
- Torii, M., Matsuzaki, F., Osumi, N., Kaibuchi, K., Nakamura, S., Casarosa, S., Guillemot, F. and Nakafuku, M. (1999). Transcription factors Mash-1 and Prox-1 delineate early steps in differentiation of neural stem cells in the developing central nervous system. *Development* **126**, 443-456.
- Truman, J. W. and Bate, M. (1988). Spatial and temporal patterns of neurogenesis in the central nervous system of *Drosophila melanogaster*. *Dev. Biol.* **125**, 145-157.
- Vaessin, H., Grell, E., Wolff, E., Bier, E., Jan, L. Y. and Jan, Y. N. (1991). prospero is expressed in neuronal precursors and encodes a nuclear protein that is involved in the control of axonal outgrowth in *Drosophila*. *Cell* **67**, 941-953.
- van Bon, B. W., Hoischen, A., Hehir-Kwa, J., de Brouwer, A. P., Ruivenkamp, C., Gijsbers, A. C., Marcelis, C. L., de Leeuw, N., Veltman, J. A., Brunner, H. G. et al. (2011). Intragenic deletion in DYRK1A leads to mental retardation and primary microcephaly. *Clin. Genet.* **79**, 296-299.
- Wallace, K., Liu, T.-H. and Vaessin, H. (2000). The pan-neural bHLH proteins DEADPAN and ASENSE regulate mitotic activity and cdk inhibitor dacapo expression in the *Drosophila* larval optic lobes. *Genesis* **26**, 77-85.
- White, K. and Kankel, D. R. (1978). Patterns of cell division and cell movement in the formation of the imaginal nervous system in *Drosophila melanogaster*. *Dev. Biol.* **65**, 296-321.
- Yabut, O., Domogauer, J. and D'Arcangelo, G. (2010). Dyrk1A overexpression inhibits proliferation and induces premature neuronal differentiation of neural progenitor cells. *J. Neurosci.* **30**, 4004-4014.
- Yao, K.-M., Samson, M.-L., Reeves, R. and White, K. (1993). Gene elav of *Drosophila melanogaster*: a prototype for neuronal-specific RNA binding protein gene family that is conserved in flies and humans. *J. Neurobiol.* **24**, 723-739.
- Zhu, L. and Skoultschi, A. I. (2001). Coordinating cell proliferation and differentiation. *Curr. Opin. Genet. Dev.* **11**, 91-97.
- Zhu, S., Wildonger, J., Barshow, S., Younger, S., Huang, Y. and Lee, T. (2012). The bHLH repressor *Deadpan* regulates the self-renewal and specification of *Drosophila* larval neural stem cells independently of Notch. *PLoS ONE* **7**, e46724.

## **SUPPLEMENTARY METHODS**

### **BrdU and EdU labeling**

For *in vivo* pulse/chase BrdU labeling experiments, recently hatched first-instar larvae were collected and grown in standard medium at 25°C. At the desired developmental time, larvae were collected again and transferred to multiwell plates and fed for 2.5 h with fruit juice containing 1 mg/ml BrdU and a red alimentary dye. Subsequently, larvae that incorporated substantial red dye in the guts were returned to standard medium to complete their development until white pupae or 24 h after adult eclosion. Larval brains were dissected in Ringer's solution and fixed for 3 min with modified Carnoy's fixative followed by 75% EtOH for 30 min. After rehydration, the samples were denatured by treatment with 2 N HCl for 40 min and then extensively washed with PBS before proceeding to IHC analysis with anti-BrdU antiserum (Beckton-Dickinson), followed with a HRP-conjugated secondary antiserum and finally revealed with DAB. To detect BrdU incorporation in adult brains, anesthetized flies were decapitated, and the heads were rapidly embedded in Tissue-Tek (Miles, Elkhart, IN) and frozen instantaneously with liquid nitrogen. Frontal 12 µm sections were obtained with a microtome cryostat and they were immediately fixed with cold 4% paraformaldehyde. After denaturation with 2 N HCl for 30 min, tissue sections were washed with PBS and processed for immunostaining with anti-BrdU as above.

*In vitro* BrdU labeling of larval brains was performed essentially as described previously (Tejedor et al., 1995; Ceron et al., 2001) but with incubation times of 5-10 min. At this end, larval brains were quickly dissected in freshly prepared Ringer solution along no more than 12 min. Eye-antenna discs were kept attached to the brains to avoid alterations in OL morphology. Brain samples were then transferred to a small well containing the BrdU (35 µ/ml) or EdU (20µM; stock: 20mM in DMSO) in Ringer's.

For BrdU detection, samples were processed as described above. For a cellular analysis, labelled larval brains were post-fixed with osmium tetroxide and embedded in SPURR, as described previously (Rogero et al., 1997). Subsequently, ultramicrotome sections (3 µm) were counterstained with 0.25% toluidine blue in 0.5% borax for 2-5 min at 60 °C, and contrasted with 75% EtOH for 5 min. These short BrdU pulses label reproducibly and strongly the OPC and CB NBs but not the IPC was not consistently labelled.

For EdU detection, after a very quick wash with Ringer solution, samples were fixed with ice cold 4% paraformaldehyde/0.1% Triton-X100 during 60min and permeabilized with PBS/0.5% Triton X-100 for 30 min at RT. Finally, they were washed with PBS/0.1% Triton X-100 just before proceeding to the Click-iT reaction (Life Technologies) under standard conditions.



## Production and purification of anti-Mnb antiserum

We raised an antiserum (called MNB-NTH) against the N-terminal region of all MNB protein isoforms following a procedure similar to that described by Tejedor et al. (1995). In brief, we produced a fusion protein by subcloning a *mnb* cDNA fragment (between Sal I and HindIII sites containing the N-terminal region of all Mnb protein isoforms) into the pGEXT-2T plasmid. The fusion protein was expressed in bacteria under standard conditions and purified by preparative SDS-PAGE electrophoresis and electroelution. The purified protein was used to immunize rabbits using standard methods. The resulting crude antiserum was affinity purified using a fusion protein prepared with the same cDNA fragment inserted into the pUR 288 expression vector. The specificity of this affinity-purified antiserum was confirmed by WB and IHC using larval brains of LoF and GoF *mnb* alleles.

## Immunohistochemistry

Larval brains were dissected in ice cold PBS along no more than 15 min. and fixed for 30 min on ice with 4% paraformaldehyde in PBS, and then for a further 30 min with 4% paraformaldehyde, 0.1% Triton X-100 in PBS. For antisera that had serious problems penetrating the tissue, larval brains were embedded in 4% low-melting-point agarose, and 50 µm sections were obtained with a vibratome. Brains or sections were saturated with incubated with primary antisera overnight at 4–8°C plus 1h at RT in PBS containing 5% normal goat serum, 0.1% Triton X-100 and 0.02% sodium azide. After extensive washing with 5 mg/ml BSA in PBS/0.1% Triton X-100, samples were incubated with Fluorescent (Alexa-488; Alexa-594, Alexa-647, Cy2, Cy3 or Cy5)-, biotin-, or HRP- coupled secondary antibodies (Jackson Immunochemicals) at 1:400–800 dilutions in 5 mg/ml BSA in PBS/0.1% Triton X-100 for 2h at RT. Cy2- or Cy3-conjugated streptavidin was used for the detection of biotinylated secondary antibodies, while labeling of HRP-conjugated secondary antibodies was revealed with Cy2, Cy3 or Cy5 TSA (Perkin Elmer). Immunolabelled samples were analyzed on Leica TCS-SL or Olympus Fluoview FV1200 confocal microscopes.

## Antibodies details.

All antibodies used in this report have been validated in previous studies.

Protein / antigen	Type	Host	Source	Reference.	Dilution
Ase	P	Rb	gift from YN Jan	Brand et al, 1993	1:2000
BrdU	M	Mo	Becton-Dickinson	Clone 3D4	1:100
Caspase3	P	Rt	Cell Signaling Tech.	Asp175	1:100
Cyc E	P	Rt	gift from H. Richardson	Crack et al., 2002	1:150
Dpn	P	Gp	gift from J. Skeath	Colonques et al, 2011	1:1500
Dpn	P	Rb	gift from YN Jan	Bier et al., 1992	1:500
Dpn	M	Rt	gift from C. Doe	Boone and Doe, 2008	1:50
DE-Cadherin	M	Rt	DSHB	Clone DCAD2	1/25
Elav	M	Rt	DSHB	Clone 7E8A10	1:200

GFP	P	Rb	Invitrogen	A11122	1:200
Grh	P	Rb	gift from H. Reichert	Bello et al., 2006	1:80
Mira	M	Mo	gift from F. Matsuzaki	Clon PLF81	1:20
Mira	P	Rb	gift from C. Gonzalez	Molinari et al., 2002	1:600
PatJ	P	Rb	gift from H. Bellen	Bhat et al., 1999	1:500
PH3	P	Rb	Upstate Biotechnology	06-570	1:500
Pros	M	Mo	DSHB	clone MR1A	1:40

Abbreviations: Gp=guinea pig, M=monoclonal, Mo=mouse, P=Polyclonal, Rb=rabbit, Rt=rat

### Analysis of cell death

In addition to TUNEL, cell death was also monitored *in vivo* in the larval brain by Acridine orange staining in freshly dissected larval brains under experimental conditions previously used in larval imaginal discs (Abrams et al., 1993). Apoptosis was also detected with anti-activated Caspase 3 antibodies (Cell Signaling Technologies). The presence of pyknotic cells was analyzed by EM. At this end, larval brains were fixed with 4% paraformaldehyde/0.5% glutaraldehyde in PBS, post-fixed with 0.2% osmium tetroxide in PBS, and embedded in SPURR. Subsequently, 2  $\mu$ m plastic sections were obtained with an ultramicrotome and stained with toluidine blue as described previously (Rogerio et al., 1997). 80–90 nm ultramicrotome sections were obtained, contrasted with uranyl acetate and lead citrate, and finally, examined using an electron microscope (JEOL USA, Inc., Peabody, MA).

### Quantitative image analysis.

For quantitative image analysis, mutant and control specimens were processed in parallel for IHC in the same experiment. Furthermore, samples were analyzed within the same work session using exactly the same acquisition parameters in the confocal microscope.

For quantitative determination of the density of labeled cells, partial projections of confocal serial sections were performed for equivalent regions (X,Y,Z axis) and counting of labeled cells was made by eye.

Quantitative determination of immune labeling intensity was carried out using the Image J program on unmodified images covering equivalent spatial regions (X,Y,Z axis) of mutant and control specimens.



## Abbreviations

BrdU, bromodeoxyuridine; CB, central brain; DAB, diaminobenzidine ; DS, Down syndrome; EdU, 5-ethynyl-2'-deoxyuridine; FISH, fluorescent in-situ hybridization; GC, ganglion cell; GMC, ganglion mother cell; GoF, gain of function; LoF, loss of function; IHC, immunohistochemistry; NB, neuroblast; NP, neural progenitor ; OL, optic lobe; OPC, outer proliferation center; PBS, phosphate buffer saline; PFA, paraformaldehyde; PH3, phosphohistone-3; RT, room temperature

## Supplementary References

Abrams JM, White K, Fessler LI, Steller H. 1993. Programmed cell death during *Drosophila* embryogenesis. *Development*. 117(1):29-43.

Almeida MS, Bray SJ (2005) Regulation of post-embryonic neuroblasts by *Drosophila* Grainyhead. *Mech Dev* 122(12): 1282–93

Bello B, Reichert H, Hirth F (2006) The brain tumor gene negatively regulates neural progenitor cell proliferation in the larval central brain of *Drosophila*. *Development* 133(14): 2639–2648.

Bier, E., Vaessin, H., Younger-Shepherd, S., Jan, L.Y., Jan, Y.N. (1992). deadpan, an essential pan-neural gene in *Drosophila*, encodes a helix-loop-helix protein similar to the hairy gene product. *Genes Dev*. 6(): 2137--2151.

Boone JQ, Doe CQ (2008) Identification of *Drosophila* type II neuroblast lineages containing transit amplifying ganglion mother cells. *Dev Neurobiol* 68(9): 1185–95.

Brand M, Jarman AP, Jan LY, Jan YN. (1993) asense is a *Drosophila* neural precursor gene and is capable of initiating sense organ formation. *Development*. 119(1):1-17.

Colonques J, Ceron J, Tejedor FJ (2007) Segregation of postembryonic neuronal and glial lineages inferred from a mosaic analysis of the *Drosophila* larval brain. *Mech Dev* 124(5): 327–40.

Colonques, J., Ceron, J., Reichert, H. and Tejedor, F. J. (2011). A transient expression of Prospero promotes cell cycle exit of *Drosophila* postembryonic neurons through the regulation of Dacapo. *PLoS One* 6, e19342.

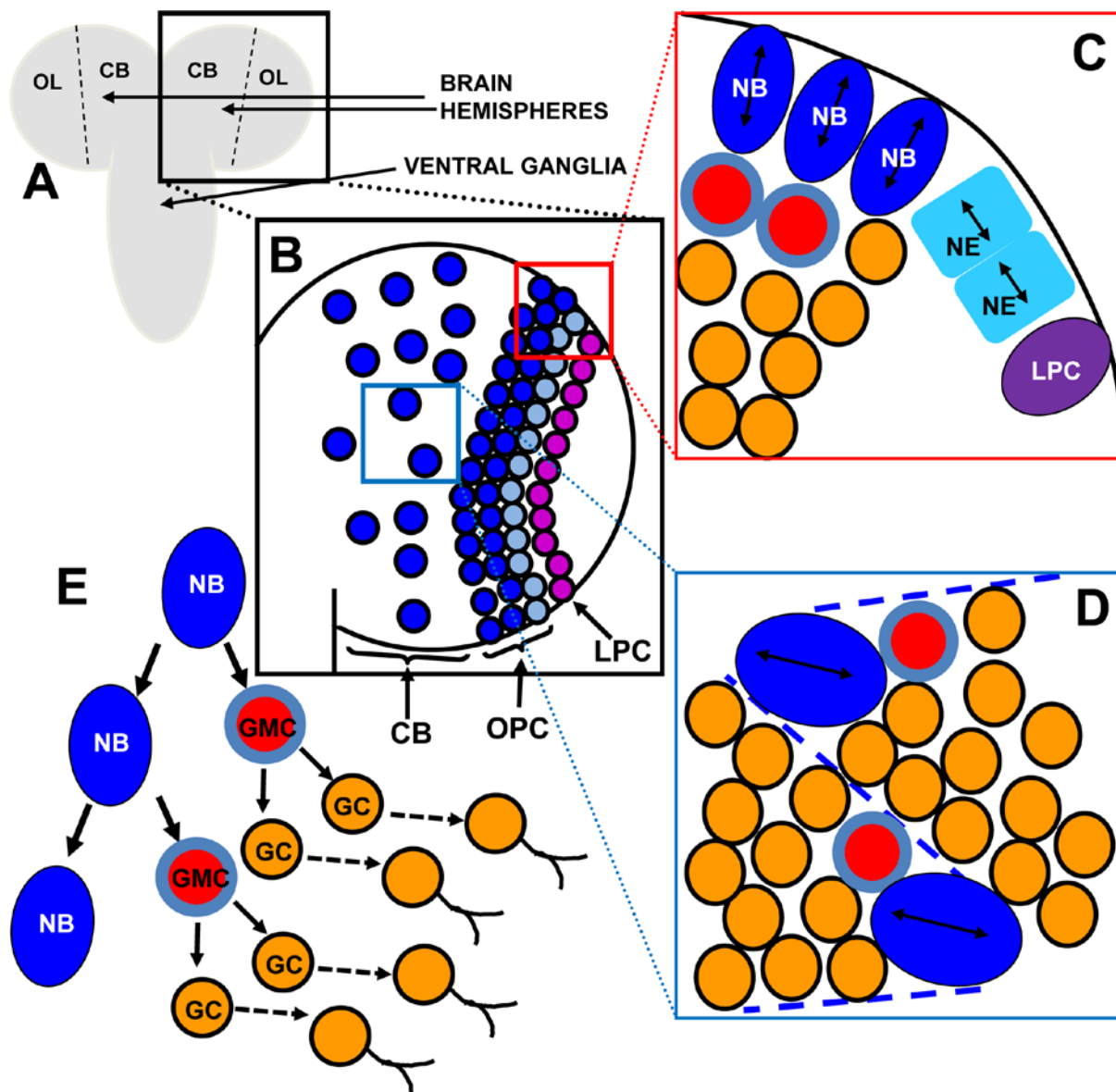
Crack D, Secombe J, Coombe M, Brumby A, Saint R, Richardson H. (2002) Analysis of *Drosophila* cyclin E1 and E2 function during development: identification of an inhibitory zone within the morphogenetic furrow of the eye imaginal disc that blocks the function of cyclin E1 but not cyclin E2. *Dev Biol*. Jan 1;241(1):157-71.

Mollinari C, Lange B, González C. (2002) Miranda, a protein involved in neuroblast asymmetric division, is associated with embryonic centrosomes of *Drosophila melanogaster*. *Biol Cell*. 94(1):1-13.

O. Rogero, B. Hammerle and F.J. Tejedor (1997) Diverse expression and distribution of Shaker potassium channels during the development of the *Drosophila* nervous system. *J. Neurosci*. 17, 5108-18

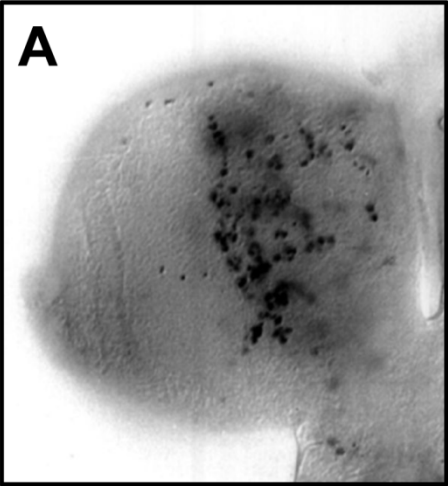
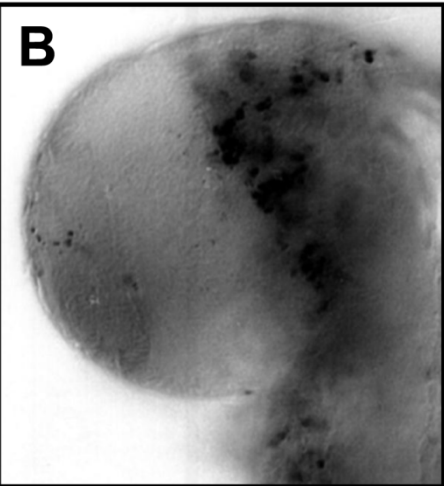
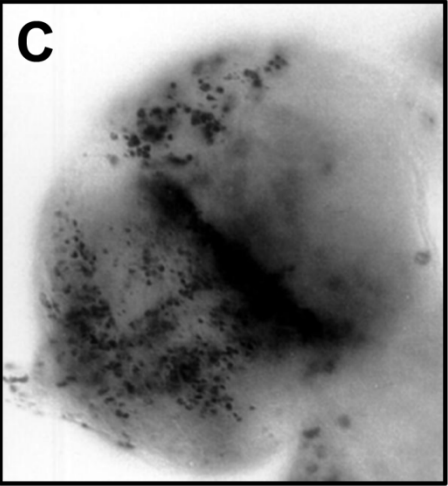
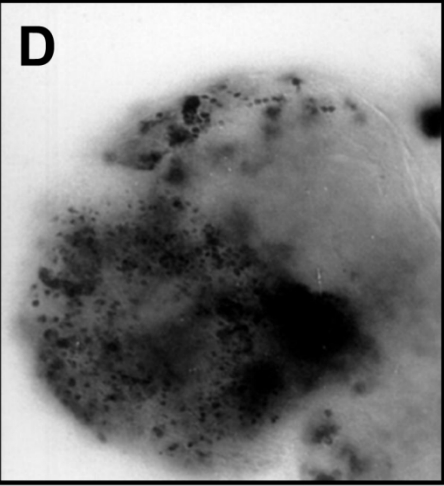
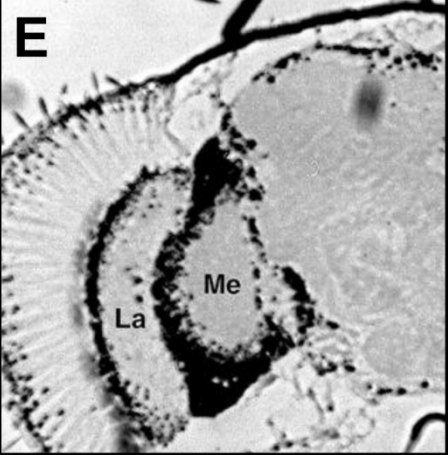
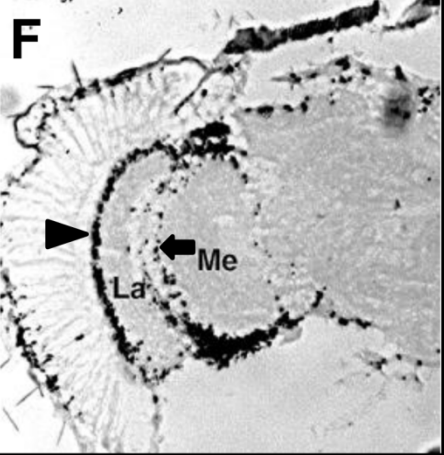
Tejedor F, Zhu XR, Kaltenbach E, Ackermann A, Baumann A, Canal I, Heisenberg M, Fischbach KF, Pongs O. (1995) minibrain: a new protein kinase family involved in postembryonic neurogenesis in *Drosophila*. *Neuron*. 14(2):287-301.





**Suppl. Fig. S1. Morphology, cellular organization and pattern of division in the larval brain hemispheres.**

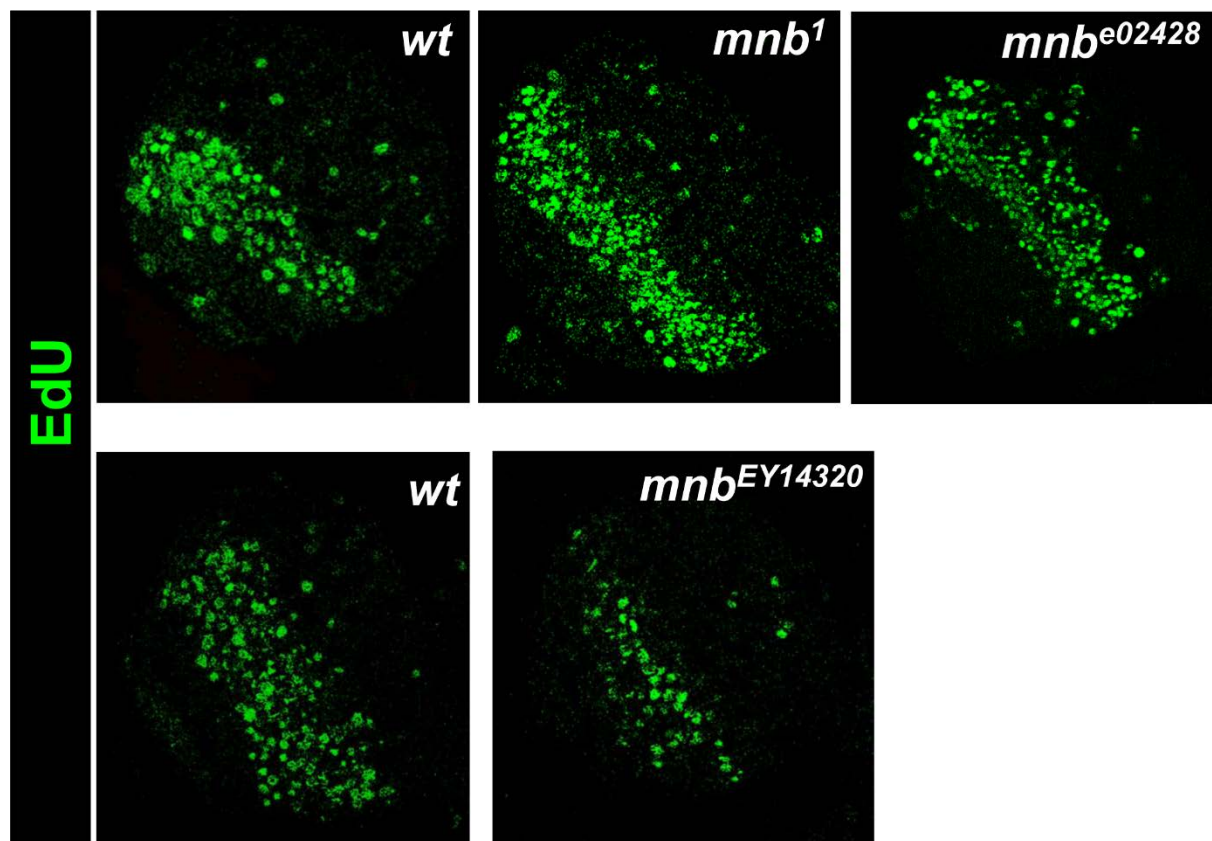
A. Schematic representation of a late larval CNS as viewed from a ventral perspective. The larval CNS is composed of two brain hemispheres and the ventral ganglia. The primordium of the adult central brain (CB) develops in the medial regions of each hemisphere, while the adult optic lobes (OL) develop from primordia located laterally. B. Schematic drawing of one hemisphere showing the scattered distribution of CB NBs in the medial part, which proliferate from the first instar stage until the beginning of pupal development, and the LPC (Lamina precursor cells) and OPC (outer proliferation center) neuroepithelia located laterally. C. Representation of the OPC showing the symmetrically dividing neuroepithelial (NE) progenitors and the asymmetrically dividing NBs, which generate their progeny inside the OL. Double arrows indicate the direction of cell division. D. Representation of two CB NBs and their progeny. E. The typical pattern of division of type I CB and OPC NBs. Each NB divides asymmetrically several times to generate in each division a new NB and an intermediate progenitor called ganglion mother cell (GMC) which divides once to generate two postmitotic ganglion cells (GCs) that differentiate into neurons.

<u>Pulse time</u>	<i>wt</i>	<i>mnb<sup>2</sup></i>	<u>Chase stage</u>
44h	<b>A</b> 	<b>B</b> 	Wand. larvae
94h	<b>C</b> 	<b>D</b> 	White pupae
110h	<b>E</b> 	<b>F</b> 	Adult 24h



**Suppl. Fig. S2. Pulse-chase BrdU labeling in *mnb* mutant.**

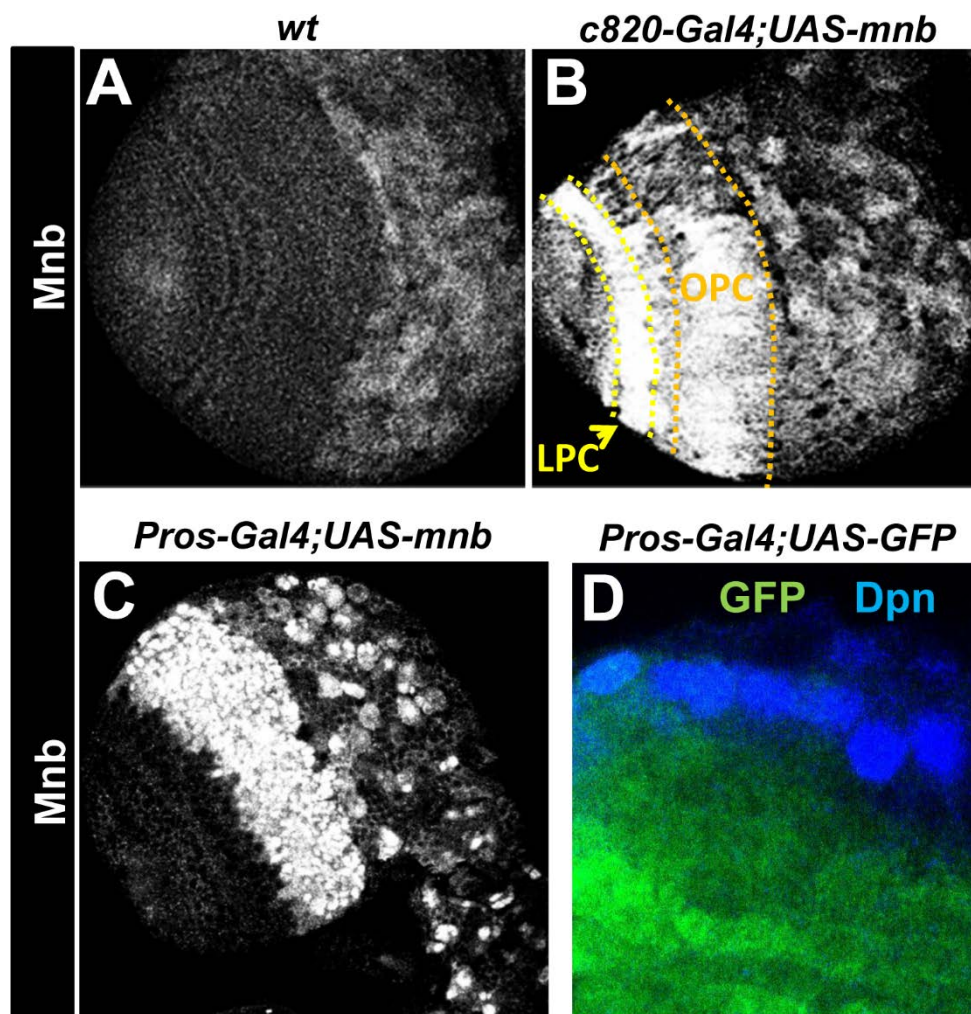
*in vivo* BrdU labeling was carried out in order to determine at which step of larval development is generated the neuronal deficit of the *mnb* mutant. A single pulse of BrdU was applied *in vivo* to *wt* and *mnb*<sup>2</sup> larvae at the indicated times of larval development. This method allows the labeling of neurons at the time of birth. BrdU incorporation was analyzed in wandering larvae (A, B), white pupae (C, D) and in one-day-old adult brain frontal sections (E, F). Note that although the brain hemispheres of *mnb* larvae do not show any decrease in BrdU immunostaining in the optic lobe (OL) or central brain (CB) regions compared with the *wt* brain, the *mnb* adult brain (a section of one brain hemisphere) displays a strong decrease in the immunolabeling of the medulla cortex (Me, arrow) compared with the equivalent *wt* section (E, F). Also note that the lamina (La) cortex (arrowhead) is less affected. This is in agreement with the morphological phenotype in the brain of adult *mnb* mutants (Fischbach and Heisenberg, 1984; Tejedor et al., 1995). These results indicate that the neuronal deficit of *mnb* flies is mainly generated during the late larval or pupal stages.



**Suppl.Fig. S3. EdU labeling of *mnb* alleles.**

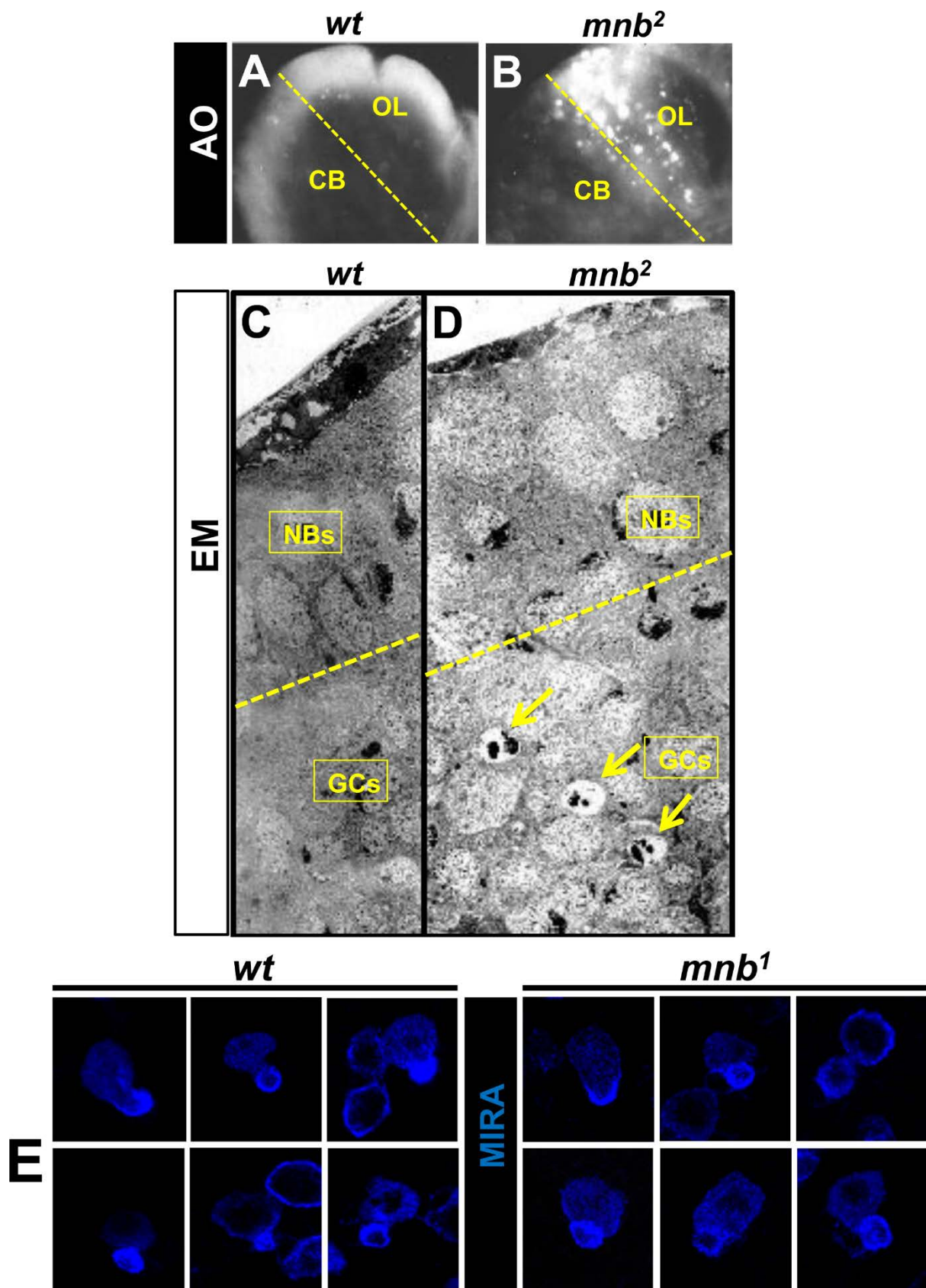
Confocal images of *wt*, *mnb<sup>1</sup>*, *mnb<sup>e02428</sup>*, *mnb<sup>EY14320</sup>* larval brains after a 7 min EdU pulse. Note the increase in EdU<sup>+</sup> cells in *mnb<sup>1</sup>*, *mnb<sup>e02428</sup>* and the decrease in *mnb<sup>EY14320</sup>*. Quantitative determination of EdU labeling is presented in Fig.1





**Suppl. Fig. S4. Expression patterns of Gal4 drivers**

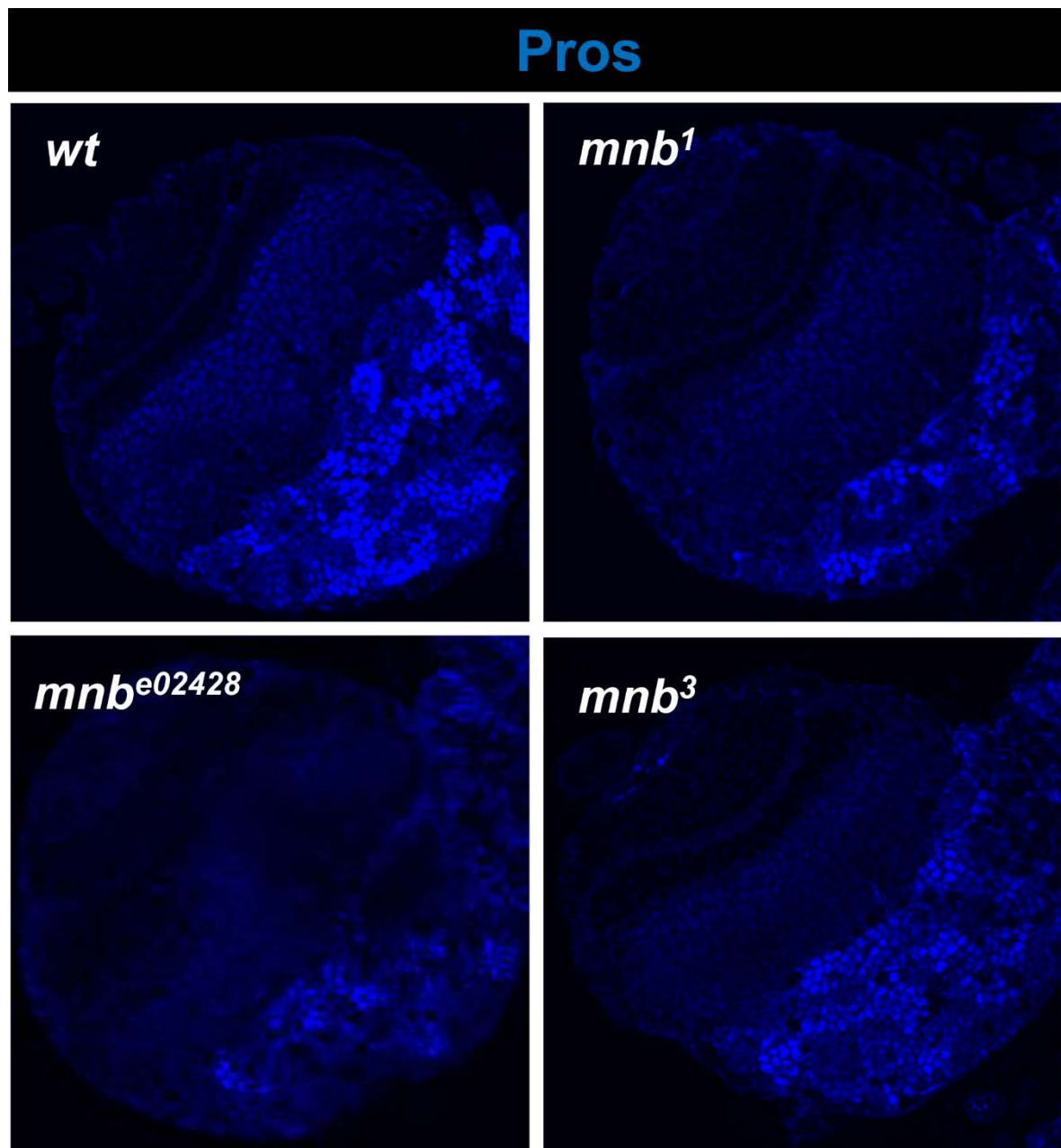
A,B,C, Confocal images taken from a ventro-anterior orientation through a brain lobe of *wt*, *c820-Gal4; UAS-mnb*, and *pros-Gal4; UAS-mnb* late third instar larvae showing Mnb immunolabeling. Note that the *c820-Gal4* driver induces strong expression of Mnb in the LPC and OPC, and moderate in some CB areas. The *pros-Gal4* driver promotes strong expression of Mnb in the OPC while in the CB is variable depending on lineage. D. High magnification view of the OPC of a *Pros-Gal4;UAS-GFP* larval brain immunostained for DPN and GFP. Note that most GFP signal is inside the OL in Dpn<sup>+</sup> cells.



**Suppl. Fig. S5. Additional cellular phenotype data of *mnb* mutants**

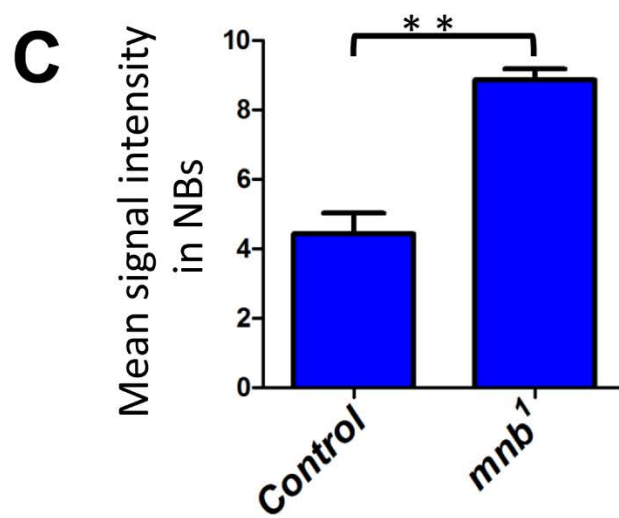
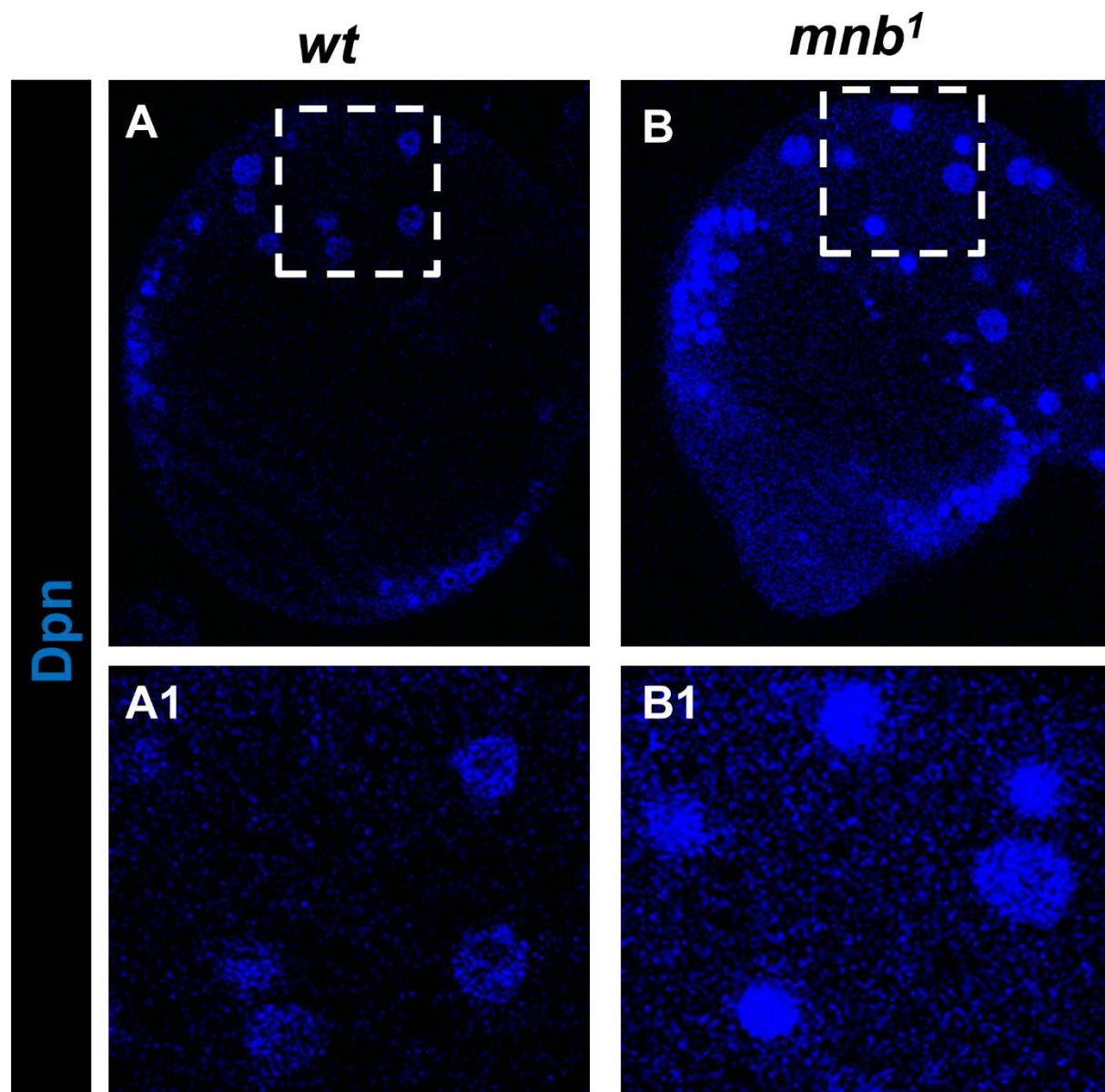
Cell death was analyzed in the OL of *mnb*<sup>2</sup> late-third-instar larvae using acridine orange (AO) staining (A, B) and electron microscopy (EM) (C,D). In the case of AO, images were obtained as projections of confocal sections through the brain lobes. Note the abundance of AO labeled cells in the *mnb* lobe compared with the wt lobe. EM images (C,D) were collected from frontal sections of larval OLs taken at the level of the OPC. Numerous pyknotic cells with fragmented and/or condensed nuclei (arrows) are located beneath the NBs in the *mnb* mutant OPC. E. High magnification views of representative CB NB lineages labelled with Mira. Note that in both *wt* and *mnb*<sup>1</sup> only one small-medium strong Mira<sup>+</sup> cell can be detected near the NB. This indicates that no apparent increase in GMCs number happens in *mnb* mutants.





**Suppl. Fig. S6. The expression of Prospero is decreased in LoF *mnbt* alleles.**

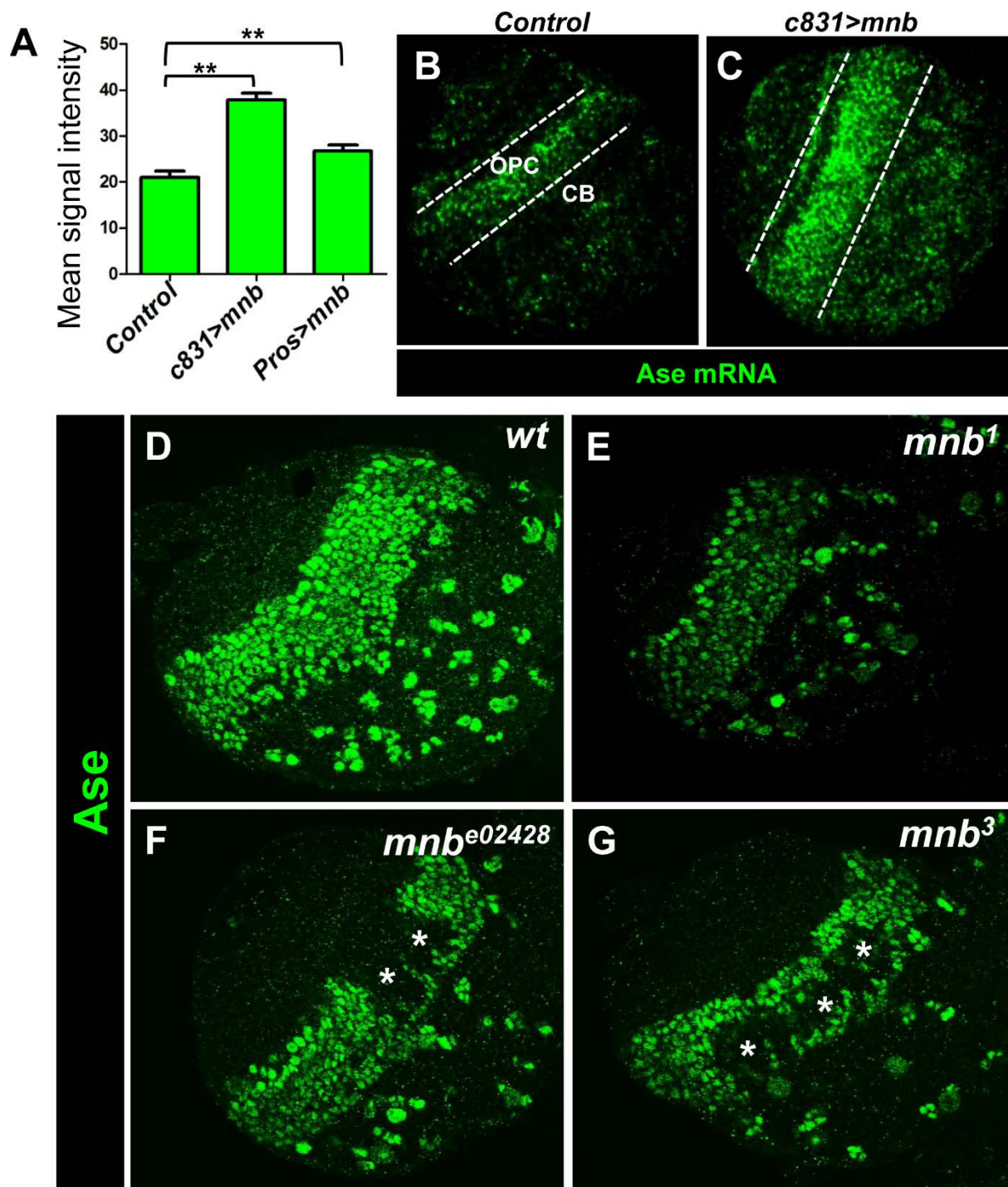
Confocal images of wt, *mnbt<sup>1</sup>*, *mnbt<sup>e02428</sup>*, *mnbt<sup>3</sup>* larval brains immunostained for Pros. Note the decreased labeling intensity in the three *mnbt* alleles. Quantification of labeling intensity is presented in Fig.5.



**Suppl. Fig. S7. The expression of Deadpan is increased in NBs of *mnb* mutant.**

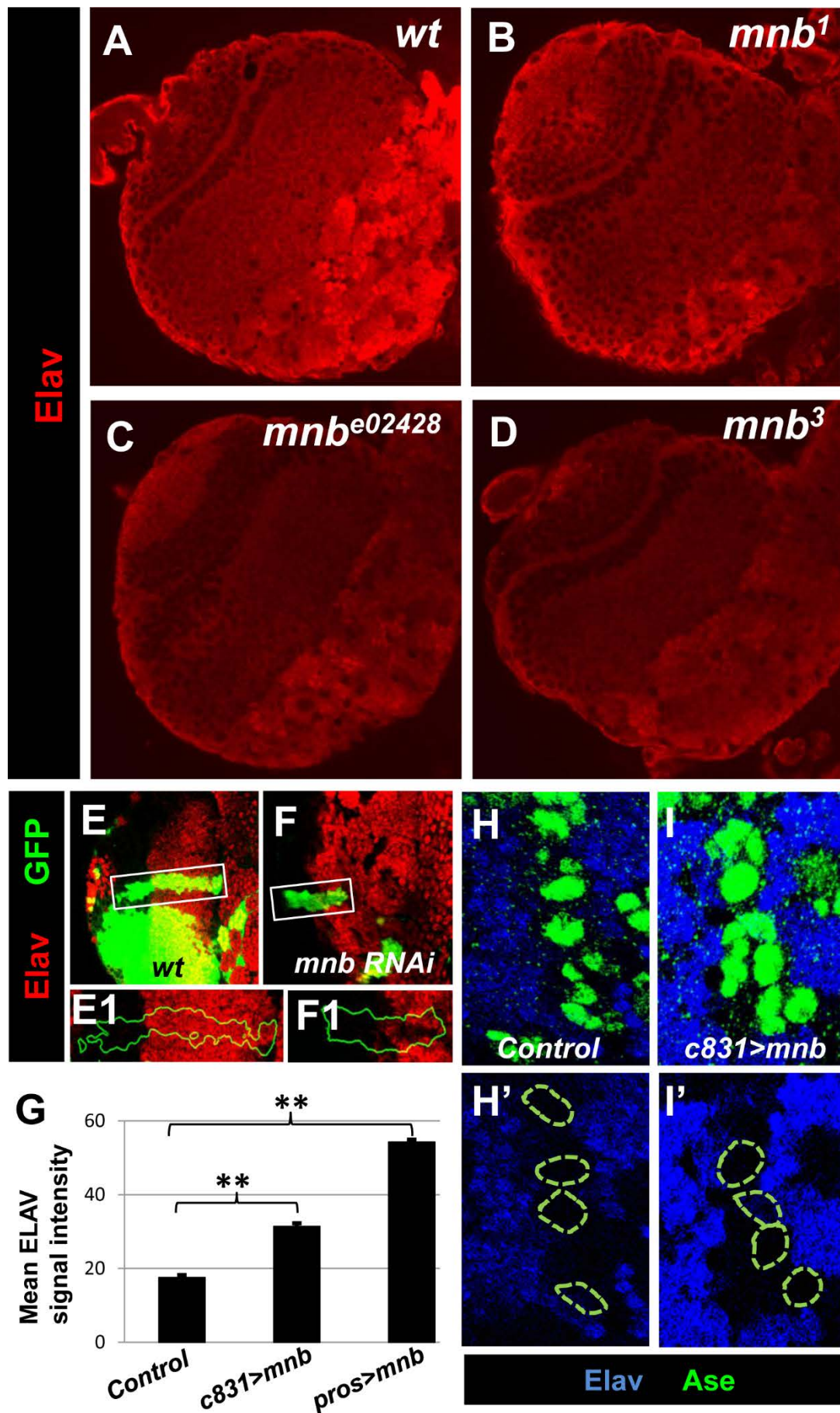
A, B. Confocal images of wt and *mnb*<sup>1</sup>, larval brains immunostained for Dpn. A1, B1. High magnification view of the framed regions in A and B. . Note the increase in labeling intensity in NBs of the *mnb* sample. Quantitative determination of labeling intensity was performed in 15 CB NBs in equivalent regions of 4 brain lobes of each genotype. Signal intensity was measured in 10µm diameter circles including each NB. (\*\*, Statistic significance,  $p < 0.0001$ ).





**Suppl. Fig. S8. Changes in the expression of Ase in *mnb* LoF and GoF mutants.**

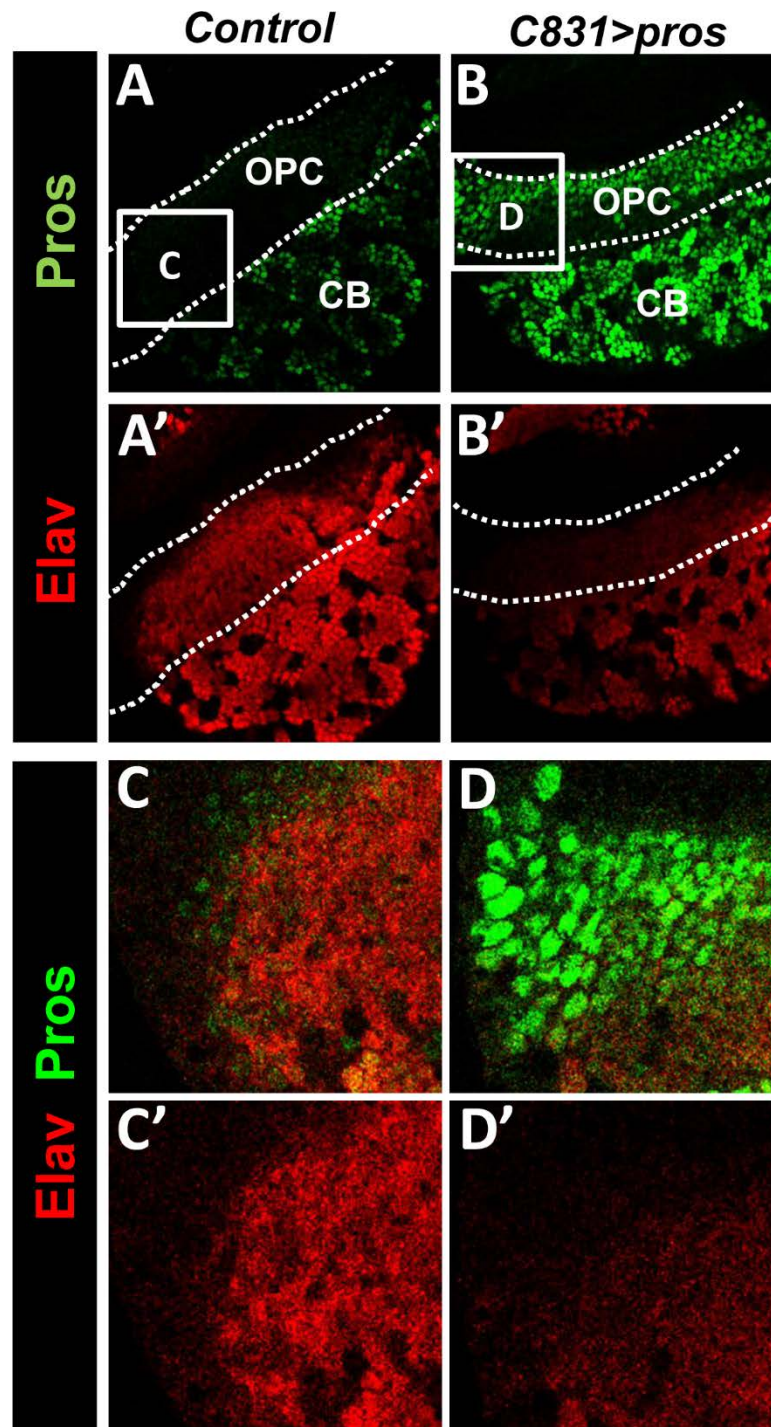
A. Quantitative determination of Ase labeling intensity was performed in 4 brain lobes of each genotype. Representative images are shown in Fig.8 (\*\*, Statistically significant,  $P < 0.0001$ ). B, C. Partial confocal projection or serial images of larval brains after FISH of Ase. Note the strong increase in labeling after driving Mnb overexpression in the OPC with c831-Gal4. D-G. Confocal images of wt, *mnb*<sup>1</sup>, *mnb*<sup>e02428</sup>, *mnb*<sup>3</sup> larval brains immunostained for Ase. Note the decreased labeling intensity in the three *mnb* alleles. In some cases, the decrease of Ase is particularly strong in some OPC cell clusters (asterisks).





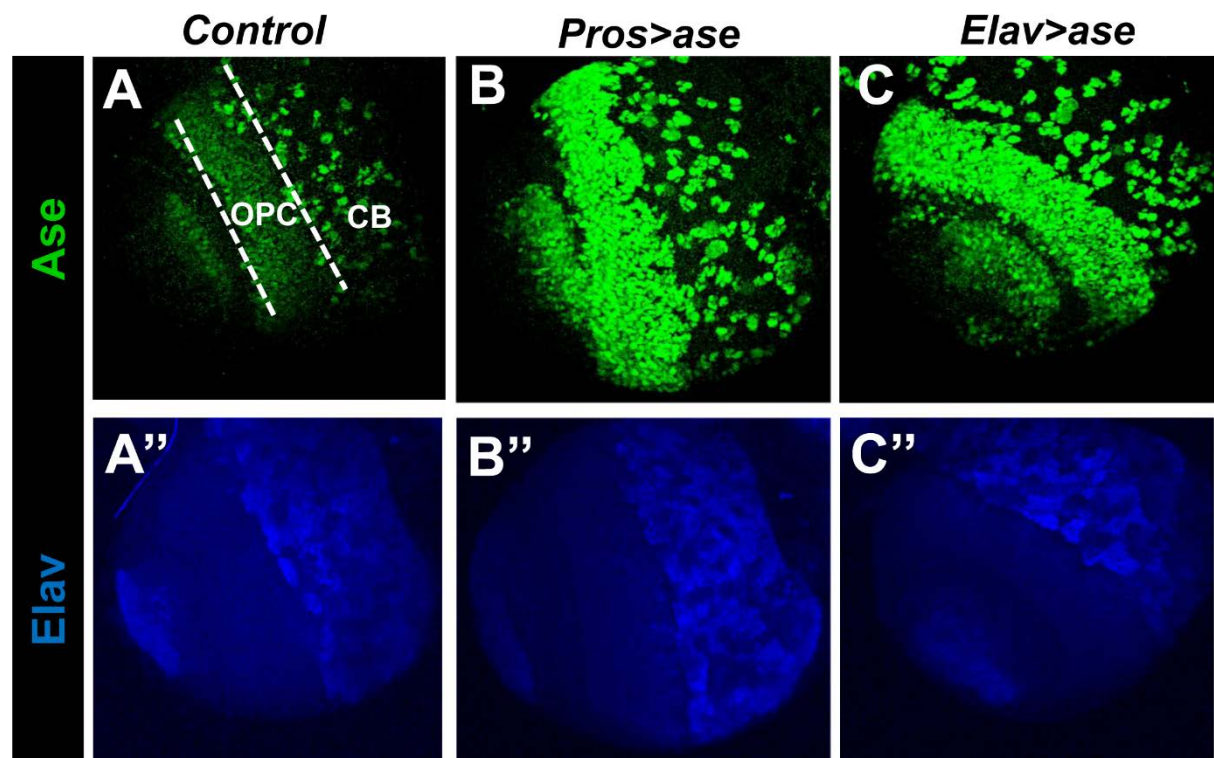
**Suppl. Fig. S9. Effects of the LoF and GoF of *Mnb* on Elav expression.**

A-D. Confocal images of *wt*, *mnb*<sup>1</sup>, *mnb*<sup>e02428</sup>, *mnb*<sup>3</sup> larval brains immunostained for Elav. Note the decreased labeling intensity in the three *mnb* alleles. E,F. Mid magnification views of the OPC of larval brains in which *wt* and *UAS-mnb RNAi* clones expressing GFP were induced. Note the decrease in Elav staining inside the *mnb* RNAi clone. G. Quantitative determination of the Elav immunostaining intensity in larval brain lobes of *UAS-mnb* (control), *c831-Gal4;UAS-mnb*, and *pros-Gal4;UAS-mnb* late-third-instar larvae. (\*\* Statistically significant,  $P < 0.001$ ). H,I. High magnification views of equivalent CB areas of *control* and *c831-Gal4; UAS-mnb* late third instar larval brains after activation at 29°C for 10h. Note the increase in Ase signal in the NBs and of Elav in the surrounding GCs. However, Elav is not elevated in NBs (dotted circles).



**Suppl. Fig. S10. Effect of the GoF of *pros* on the expression of Elav.**

A,B. Partial confocal projection images taken from a ventro-anterior orientation through the lobe of wt and *c831-Gal4; UAS-pros* late third instar larvae showing Pros and Elav immunolabeling. Note the increase in Pros level in the mutant OPC accompanied by some decrease in Elav. C,D. High magnification view of a single confocal section of the corresponding OPC areas framed in A and B, respectively. Notice the decrease in Elav in those cells with strong Pros labeling. This indicates that Pros might exert a suppression on *elav* expression. Nevertheless, we can not rule out that the decrease in Elav level could be an indirect effect due to the proliferation arrest of NBs and concomitant inhibition of neurogenesis that the GoF of *pros* causes (Colonques et al., 2011).



**Suppl. Fig. S11. Effects of the GoF of Ase on Elav expression**

A-C. Partial confocal projection images taken from a ventro-anterior orientation through the lobe of *Control*, *pros-Gal4;UAS-ase* and *elav-Gal4;UAS-ase* late third instar larvae showing Ase and Elav immunolabeling. Note that the strong induction of Ase both in the CB and OPC of the mutant lobes does not cause substantial changes in Elav labeling.



**Supplementary Table S1. Information of *mnb* alleles**

Allele	Genetic and Molecular nature	Phenotypes	Literature
<i>mnb</i> <sup>1</sup>	Null  Point mutation in kinase active site	Adult brain morphology  BrdU labeling  Cell death Expression of Cyclins Expression of Ase, Pros, Dap, Dpn, and Elav	Fischbach and Heisenberg, 1984  Tejedor et al, 1995  This paper
<i>mnb</i> <sup>2</sup>	Strong hypomorph  P-element insertion	Adult brain morphology  BrdU labeling  Cell death Expression of Cyclins Expression of Ase, Pros, Dap, Dpn, and Elav	Fischbach and Heisenberg, 1984  Tejedor et al, 1995  This paper
<i>mnb</i> <sup>3</sup>	Strong hypomorph	Adult brain morphology BrdU labeling  Expression of Ase, Pros, and Elav	Tejedor et al, 1995  This paper
<i>mnb</i> <sup>e02428</sup>	P-element insertion  Strong hypomorph	EdU labeling Cell death Expression of Ase, Pros, and Elav	Parks et al., 2004; Thibault et al., 2004  This paper
<i>mnb</i> <sup>EY14320</sup>	P-element insertion  Mnb overexpression	EdU labeling Expression of Cyclins	Bellen et al., 2004  This paper

**References:**

Bellen et al., 2004, Genetics 167(2): 761—781

Parks et al., 2004, Nat. Genet. 36(3): 288—92

Thibault et al., 2004, Nat. Genet. 36(3): 283--287 [